CHARLES UNIVERSITY IN PRAGUE

FACULTY OF PHARMACY IN HRADEC KRÁLOVÉ

Department of Pharmacognosy

UNIVERSITÉ D'ANGERS

DÉPARTEMENT PHARMACIE

SONAS (Équipe Substances d'origine naturelle et analogues structuraux)

Toward new analogues of vitamin E: new potential inhibitors of 5-lipoxygenase

Diploma thesis

Supervisors: Jean-Jacques Helesbeux, PhD.
doc. PharmDr. Lenka Tůmová, PhD.

Hradec Králové, September 2019 Martina Štůsková

DECLARATION

"I, Martina Štůsková, hereby declare that this diploma thesis is my original work. All used literature and sources are listed in the list of used literature at the end of the thesis and properly cited. This works has not been used to gain equal or different academic degree."

Hradec Králové, September 2019 Martina Štůsková

ACKNOWLEDGEMENT

I would like to thank the research group SONAS of University of Angers, especially Jean-Jacques Helesbeux, PhD., for letting me become part of his research group. Significant thanks belong to my consultant, Allexia Ville, PhD., for all her help, guidance and patience.

For her advice and a lot of useful comments, I would like to thank doc. PharmDr. Lenka Tůmová, PhD.

Content

List of Abbreviation 7

List of Figures 8

List of Tables 9

List of Charts 9

I. Introduction 10

II. Aim of the thesis 12

III. Theoretical part 13

1 Vitamin E 13

1.1 Biosynthesis of tocopherols and tocotrienols 14

1.2 Metabolism of vitamin E in the human body 15

1.3 Natural sources of vitamin E 18

1.3.1 The main sources of tocotrienols and their analogues 19

1.4 Biological properties of vitamin E 24

1.4.1 Antioxidant activity 24

1.4.2 Inhibition of cholesterol biosynthesis 25

1.4.3 Cardioprotective activity 25

1.4.4 Anticancerogenic effect 26

1.4.5 Neuroprotective effect 26

1.4.6 Anti-inflammatory effect 27

2 Inflammation 29

2.1 Arachidonic acid metabolism 29

2.1.1 Cyclooxygenase pathway 31

2.1.2 Lipoxygenase pathway 33

IV. Experimental part 37

1 Chemicals 37

2 Materials and methods 38
3 Purification of crude extract of *Bixa orellana* 39
4 Protection of δ-T3 39
5 Metathesis reaction 41
5.1 Olefin methatesis 42
5.1.1 Types of olefin metathesis 43
5.1.2 Catalysts of CM olefin metathesis 44
5.2 HPLC analysis 46
5.3 Reaction under microwave irradiation 47
6 Deprotection of p2-p4 products 48
7 Additional reactions 50
7.1 4-pentenoic acid 50
7.2 Tosylated methyl ester of δ-garcinoic acid + methacrylate 51
7.3 2-methylenepropane-1,3-diyl diacetate 53
V. Results of optimization 56
1 Results according to the type of catalyst 56
1.1 Yields of products with Grubbs catalyst Ru-2 56
1.2 Yields of products with Grubbs catalyst Hg-1 57
1.3 Yields of products with Grubbs catalyst Hg-2 57
2 Yields of products after 1day reaction 59
3 Reaction in a microwave reactor 60
VI. Discussion and Conclusion 62
VII. Organic synthesis 64
TsOδT3 64
General procedure for the Grubbs metathesis to δT3 derivatives 65
General procedure of deprotection of new δT3 derivatives 67
Appendix 71

1 Chromatograms of standards 71
2 Chromatogram of the highest yield of all products 72
3 Chromatograms of balanced ratio of products 73
4 Table of all performed metathesis reactions during optimization. 74
References 75

List of Abbreviation

α-TTP	α-tocopherol-transfer protein
AA	Arachidonic acid
Ac	Acetone
GA	Garcinoic acid
atm	Atmospheric pressure
CAM	Cerium Ammonium Molybdenum stain
COX	Cyclooxygenase
CVD	Cardiovascular disease
DCM	Dichloromethane
HPLC	High performance liquid chromatography
IPA	Isopropanol
LOX	Lipoxygenase
LT	Leukotrienes
MA	Methacrylate
NMR	Nuclear magnetic resonance
PE	Petroleum ether
PG	Prostaglandins
RM	Reaction mixture
SONAS	Équipe Substances d'origine naturelle et analogues structuraux (Natural Substances and Structural Analogues Group)
T	Tocopherol
THF	Tetrahydrofuran
TLC	Thin-layer chromatography
TNF	Tumor necrosis factor
T3	Tocotrienol
VE	Vitamin E

List of Figures

Figure 1: Isoforms of vitamin E. 13
Figure 2: Biosynthesis of tocotrienols and tocopherols. 15
Figure 3: Vitamin E secretion in chylomicrons and distribution to circulating lipoproteins. 16
Figure 4: Metabolism of tocopherols and tocotrienols. 17
Figure 5: *Bixa orellana L.:* The tree and seeds in capsule. 19
Figure 6: Rice grains with husk and completely refined rice grains. 21
Figure 7: Nuts of *G.kola.* 22
Figure 8: New oxidized T3 derivatives found by Terashima et al. 22
Figure 9: Structures of two major secondary metabolites isolated from the barks of *G. amplexicaulis* 23
Figure 10: *Garcinia amplexicaulis* shrub. 23
Figure 11: Antioxidant activity of VE. 24
Figure 12: Basic scheme of arachidonic acid pathway. 30
Figure 13: (A) 3D structure of the 5-LOX; (B) Coordination of Fe^{2+} (orange bead) in the active site of 5-LOX according to Gilbert et al. 33
Figure 14: Chemical structure of zileuton. 34
Figure 15: Synthesis of the tosylated δ-T3. 40
Figure 16: Metathesis reaction. 41
Figure 17: Olefin metathesis. 43
Figure 18: General catalytic cycle of olefin metathesis. 43
Figure 19: Structure of catalysts used in metathesis reaction. 46
Figure 20: Illustration of the two main dielectric heating mechanisms: dipolar polarization and ionic conduction. 48
Figure 21: Scheme of two-step deprotection. 49
Figure 22: Scheme of the reaction with 4-pentenoic acid. 50
Figure 23: Scheme of esterification of 4-pentenoic acid. 51
Figure 24: Scheme of protection of δ-GA-ME. 52
Figure 25: Scheme of reaction of δTsO-GA-ME with methacrylate. 52
Figure 26: Scheme of synthesis of 2-methylenepropane-1,3-diyl diacetate. 53
Figure 27: Scheme of di-Mannich reaction. 53
Figure 28: Scheme of reduction. 54
Figure 29: Scheme of tosylation of αT3. 54
Figure 30: Scheme of reaction of TsOαT3 with 2-methylene-1,3-propanediol. 55

List of Tables

Table 1 The contents of tocopherols and tocotrienols (mg/100 g of oil) in some common edible oils. 18
Table 2: Several examples of natural redox-active inhibitors of 5-LOX. 35
Table 3: Variables of the reaction. 41
Table 4: Types of olefin metathesis..... 44
Table 5: Comparison of estimated yields – Ru-2 catalyst. 56
Table 6: Comparison of estimated yields – Hg-1 catalyst. 57
Table 7: Comparison of estimated yields – Hg-2 catalyst. 57
Table 8: Comparison of estimated and real yield after 1 day, 2.4 eq. of MA. 59
Table 9: Estimated yields – reaction in a microwave reaction. 60
Table 10 and chromatogram 1: Starting compound – TsOδT3. 71
Table 11 and chromatogram 2: Product p2. 71
Table 12 and chromatogram 3: Product p3. 71
Table 13 and chromatogram 4: Product p4. 72
Table 14 and chromatogram 5: 3-days reaction MS14..... 72
Table 15 and chromatogram 6: 1-hour reaction MS45..... 73
Table 16 and chromatogram 7: 3-days reaction MS19..... 73
Table 17: A summary of all metathesis reactions performed during optimization. 74

List of Charts

Chart 1: Comparison of the highest yields – 2.4 eq. of MA, 3 days..... 58
Chart 2: Comparison of the yields – 1.2 eq. of MA, 3 days. 58
Chart 3: Comparison of estimated and isolated yields after 1day reaction with 2.4 eq. of MA. 59
Chart 4: Comparison of estimated yields – reaction in a microwave reactor. 60

I. Introduction

Inflammatory diseases are a major cause of various public health problems such as asthma, allergies, and arthritis. For example, the number of asthma sufferers in the world has increased from 150 million in 2002 to 339 million in 2018.[1] Inflammation is also involved in the development of cardiovascular diseases, certain cancers, Alzheimer's disease and many other pathologies. It results from overreacting immune response and is characterized by the production of a multitude of proinflammatory mediators, including lipid mediators, notably prostaglandins and leukotrienes, and cytokines such as TNF-α and interleukin-6, which in turn aggravate inflammation and lead to excessive damage to host tissues. If this process is poorly controlled and persists over time, a chronic inflammation stage is set up and can participate in the development of certain diseases. Two key players are important during these inflammatory processes: cyclooxygenase (COX) and 5-lipoxygenase (5-LOX) enzymes which catalyze the oxidation of arachidonic acid (AA) into prostaglandins (PG) and leukotrienes (LT). The most commonly used therapeutic strategies to fight inflammation aim to inhibit the biosynthetic pathways of these proinflammatory mediators. Non-steroidal anti-inflammatory drugs and steroids are the most common drugs used to treat inflammation. Many side effects occur with long term treatment, in particular gastrointestinal side effect is a major side effect associated with the currently available non-steroidal anti-inflammatory drugs which limit their application.[2, 3]

In 2012, SONAS (Équipe Substances d'origine naturelle et analogues structuraux) was associated to the DNTI project (Drugs from Nature Targeting Inflammation) whose goal was to find new molecules of natural origin targeting inflammation. This project allowed the pooling of the know-how of different laboratories: Among them, there was the laboratory of Prof. Stuppner of the University of Innsbruck (Austria) that has skills in molecular modeling; laboratory of Prof. Richomme (SONAS) of the University of Angers is specialized in the chemistry of natural products; and finally the laboratory of Prof. Werz (Jena, Germany) intervened to carry out the biological evaluations *in vitro, in cellulo* and the general lipidomic studies.

[1] World Health Organization, *Implementation of the WHO strategy for prevention and control of chronic respiratory diseases: meeting report, 11-12 February 2002*, Geneva: World Health Organization, 2002.

In the frame of the phytochemical study of an endemic plant from New Caledonia, *Garcinia amplexicaulis*, the SONAS laboratory isolated and identified several original oxidized tocotrienols (T3). These are analogues of vitamin E (VE) for which the broad spectrum of biological activities is widely documented in scientific literature. *In silico* screening of these vitamin E analogues with several enzymatic targets involved in inflammatory processes has been carried out by our Austrian colleagues. As a result of this study, 5-LOX has been identified as a primary target for T3 derivatives. As part of our collaboration with Prof. Werz's team, many T3 derivatives were submitted to biological testing. Thus, the inhibition of the enzymatic activity (IC_{50}) of 5-LOX was evaluated on purified enzyme and PMNL cells (polymorphonuclear leucocytes), true reservoirs of this enzyme. PMNLs account for 50 % to 70 % of white blood cells and are among the first cells to migrate in large numbers to the site of inflammation, making it one of the essential elements of pathogen defence.

My thesis will focus on the semisynthesis and its optimization of new analogues of T3 to better understand and extend the library of possible 5-LOX inhibitors and then verification of the reaction conditions with another T3 analogues.

The first chapter will present the general context of this thesis subject and it will be devoted to vitamin E and its derivatives: history, structure, natural resources, varied biological activities etc. Then, the second part will deal with inflammation by describing generalities about this physiological phenomenon, the pro-inflammatory mediators involved, as well as the different known inhibitors and their targets in this complex process.

The second chapter will describe the strategy developed during the thesis and its specification. At first, the extraction and purification of crude extract of *Bixa orellana*, leading to δT3 the precursor for most semisynthesis work, was carried out. Then, the optimization of semisynthetic reaction using this as starting material will be described and its analysis by HPLC chromatography will be explained. Consequently, the optimal conditions were studied with reactions using other derivatives of tocotrienol and their applicability was observed.

New analogues of VE synthesized during my work have been or will be tested *in vitro* on purified 5-LOX and PMNL by our German colleagues in Jena.

II. Aim of the thesis

The main aims of my thesis are:

1. To optimize the reaction conditions to access potential new 5- lipoxygenase inhibitors based on δ-tocotrienol, which is obtained from crude extract of *Bixa oreallana.*

2. To find an efficient way of deprotection to lead to the final molecules.

3. To verify and apply the effective conditions of semisynthesis and synthesize additional potential inhibitors of 5-lipoxygenase from other T3 derivatives.

III. Theoretical part

1 Vitamin E

The discovery of vitamin E (VE) is dated to 1922 when Herbert Evans and Katherine Scott Bishop described a formerly unrecognized substance called “antisterility factor x” founded in green leafy vegetables, which was required to be indispensable for reproduction of rats. [1,2] Once identified, it was referred as containing tocopherols; the term is based on the Greek words *tokos*, which means “offspring” and *phero*, which means “to bear, to carry.” Therefore, tocopherol means “to bear children”. [3] Over the time other functions and properties of vitamin E were observed: antioxidant activity, essential factor for the development of tissues and organs such as brain and nerves, muscle and bones, skin, etc. [3] Actually, tocotrienols attracted no real attention until the late 1980’s and 1990’s when their cholesterol-lowering potential and anticancer effects were first described. [4]

Today vitamin E is a generic name for the family of eight major lipophilic compounds that have been found to carry the vitamin E activity. The compounds are divided into two groups: tocopherols (T) and tocotrienols (T3). [6] All vitamin E forms have a chroman-6-ol ring bearing a 16-carbon side chain in chiral position C2 with a *R* configuration. [5] Tocopherols are characterized by a saturated phytyl-like side chain with 2 chiral carbons (in position 4' and 8'), whereas tocotrienols have a farnesyl-like side chain with double bonds at carbons 3', 7' and 11'. [2] Isoforms of tocopherol and tocotrienol differ at the 5- and 7- position on chroman-6-ol ring with either an H or a CH_3 group (they are referred to as α, β, γ, and δ form). [5]

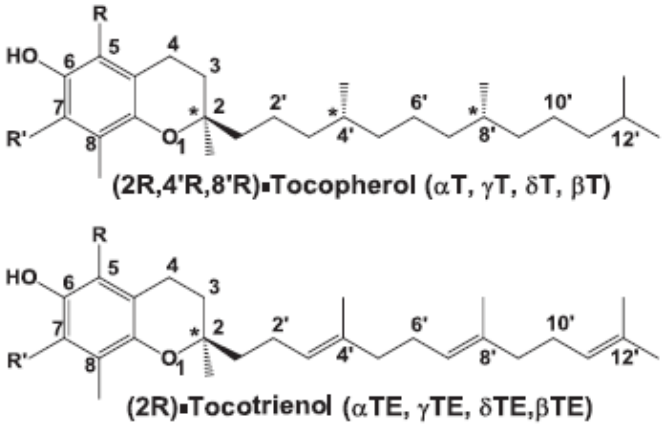

Isoforms	*R*	*R′*
α	CH_3	CH_3
β	CH_3	H
γ	H	CH_3
δ	H	H

Figure 1: Isoforms of vitamin E. [5]

1.1 Biosynthesis of tocopherols and tocotrienols

Tocopherol biosynthesis is initiated in the plant's cytoplasm, but, except for this first step, its biosynthesis takes place in the plastids. [6] The biosynthesis starts through the formation of the aromatic head group homogentisic acid (HGA), which is catalyzed by the enzyme p-hydroxyphenylpyruvate and is derived from tyrosine degradation. [7] The polyprenyl side chain, phytyl diphosphate (PDP), is suggested to originate from the DOXP (non-mevalonate) pathway, as well as from the recycling of free phytol derived from the process of chlorophyll degradation. [6] The two substrates, HGA and PDP, are fused together in the following step, mediated by the enzyme homogentisate phytyltransferase (HPT), to 2-methyl-6-phytyl-1,4-benzoquinol (MPBQ). MPBQ, in turn, serves as substrate either for tocopherol cyclase (TC) or MPBQ methyltransferase. MPBQ methyltransferase methylates MPBQ to 2,3-dimethyl-6-phytyl-1,4-benzoquinone (DMPBQ), while tocopherol cyclase transforms both MPBQ and DMPBQ to γ- and δ-tocopherol, respectively. Lastly, the enzyme γ-tocopherol methyltransferase (γ-TMT) catalyzes the conversion of γ- to α-tocopherol and of δ- to β-tocopherol. [6-9]

Tocotrienol biosynthesis is believed to involve reactions analogous to those associated with tocopherol biosynthesis. [8] The only difference is that the initial condensation reaction is presumed to use geranylgeranyl diphosphate (GGDP) instead of PDP, given the similarity in unsaturation between GGDP and the hydrocarbon chain of tocotrienols. [7,8]

The major reason why plants synthesize tocochromanols appears to be for antioxidant activity. Different parts of plants, and different species, are dominated by different tocochromanols. The predominant form in leaves, and hence leafy green vegetables is α-tocopherol. [6] They are located in chloroplast membranes, this in close proximity to the photosynthetic process. [9] The function is to protect against damage from the ultraviolet radiation of sunlight. Under normal growing conditions the presence of α-tocopherol does not appear to be essential, as there are other photo-protective compounds, and plant mutations that have lost the ability to synthesize α-tocopherol demonstrate normal growth. [10] However, under stressed growing conditions such as drought, elevated temperature or salt-induced oxidative stress, the plants' physiological status is superior if it has the normal tocopherol synthesis capacity. [6,10]

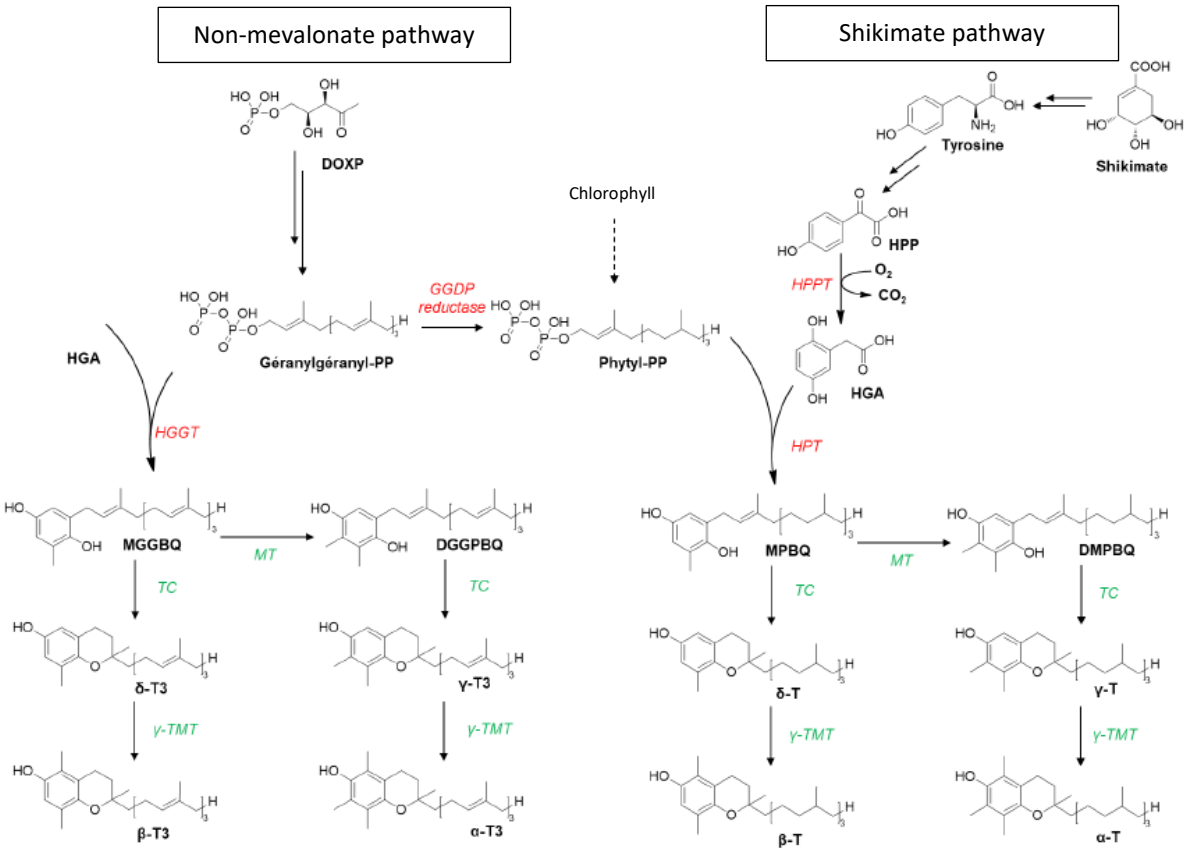

Figure 2: Biosynthesis of tocotrienols and tocopherols. [11]

1.2 Metabolism of vitamin E in the human body

The uptake of VE into plasma is similarly absorbed to dietary fat uptake through the small intestine due to its high lipophilicity. Bile and pancreatic acid secretions in the intestinal lumen help in forming micelles containing VE and lipid hydrolysis products which are absorbed through the membrane of intestinal cells and transported through lipoproteins especially by chylomicrons in the lymph and blood. [5,12] In the gastro-intestinal system the absorption rate of vitamin E varies interindividually between 20 % - 80 %. [13] The chylomicron-bound vitamin E forms are transported to the peripheral tissues, including muscle, bone marrow, adipose tissue, skin, and possibly brain. In these tissues, vitamin E forms are picked up by a lipoprotein receptor-mediated process, which is not well understood yet. [5]

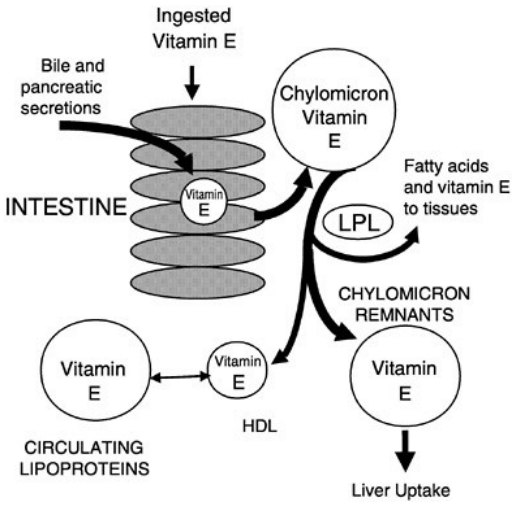

Figure 3: Vitamin E secretion in chylomicrons and distribution to circulating lipoproteins. [14]

The liver takes up chylomicron remnants and secretes VLDL into circulation. Studies using deuterated tocopherols indicated that *RRR*-α-tocopherol is preferentially secreted by hepatocytes. [15] Cellular vitamin E is specifically bound to intracellular transport proteins, such as hepatic α-tocopherol-transfer protein (α-TTP) in the liver where this protein is highly expressed. [5,13] α-TTP is a cytosolic protein with a molecular weight of 32 kDa coded by a gene located on chromosome 8. [13] It is a member of the CRAL-TRIO family, which consists of lipid-binding proteins in control of intracellular trafficking of hydrophobic molecules. It was found and identified in hepatocytes, human brain and human placenta. Crystallographic studies revealed that α-tocopherol is bounded by α-TTP inside a hydrophobic pocket through van der Waals contacts. Inside the hydrophobic pocket there are also four hydrophilic molecules: two are hydrogen-bonded to the hydroxyl group of the chromanol ring, one is hydrogen-bonded to the oxygen atoms of Val182 and Leu189, and the fourth hydrophilic molecule is hydrogen-bonded to the hydroxyl group of the Ser140. [5,13-15] Requirements for the binding of VE isoforms and derivatives to α-TTP are: the methylation degree of the chromanol ring system (especially at position C5), one free hydroxyl group and the phytyl side chain, and the *R* configuration at C2 where the phytyl tail is linked to the chromanol ring. [13,15] The affinity of different vitamin E forms to α-TTP is dissimilar: *RRR*-α-T set to 100%, other isoforms and stereoisomers are just among 2-38% affinity. [5,13] The almost zero affinity of tocotrienols to α-TTP is induced by the presence of the three double bonds with rigid configurations, which hinder the unsaturated tail to appropriately accommodate in the hydrophobic pocket of the protein. [13-15] *RRR*-α-tocopherol is preferentially resecreted by the liver and distributed to circulating lipoproteins. [14]

Unlike other fat-soluble vitamins, VE is not stored in the human body. [14] The metabolism of VE vitamers consists of an initial ω-hydroxylation. The hydroxyl group is oxidized to a carboxyl group. The final step is represented by a sequence of β-oxidation degrading to α-, β-, γ-, and δ-CEHC (2'-carboxyethyl-6-hydroxychromane), that involves shortening the phythyl tail of the molecules, and after either sulphatation or glucuronidation. [14] The chromanol ring stays unchanged. The metabolites are formed in endoplasmatic reticulum, peroxisome and mitochondria. The molecules become more water-soluble and leads to urine excretion. [14,15] (Figure 4)

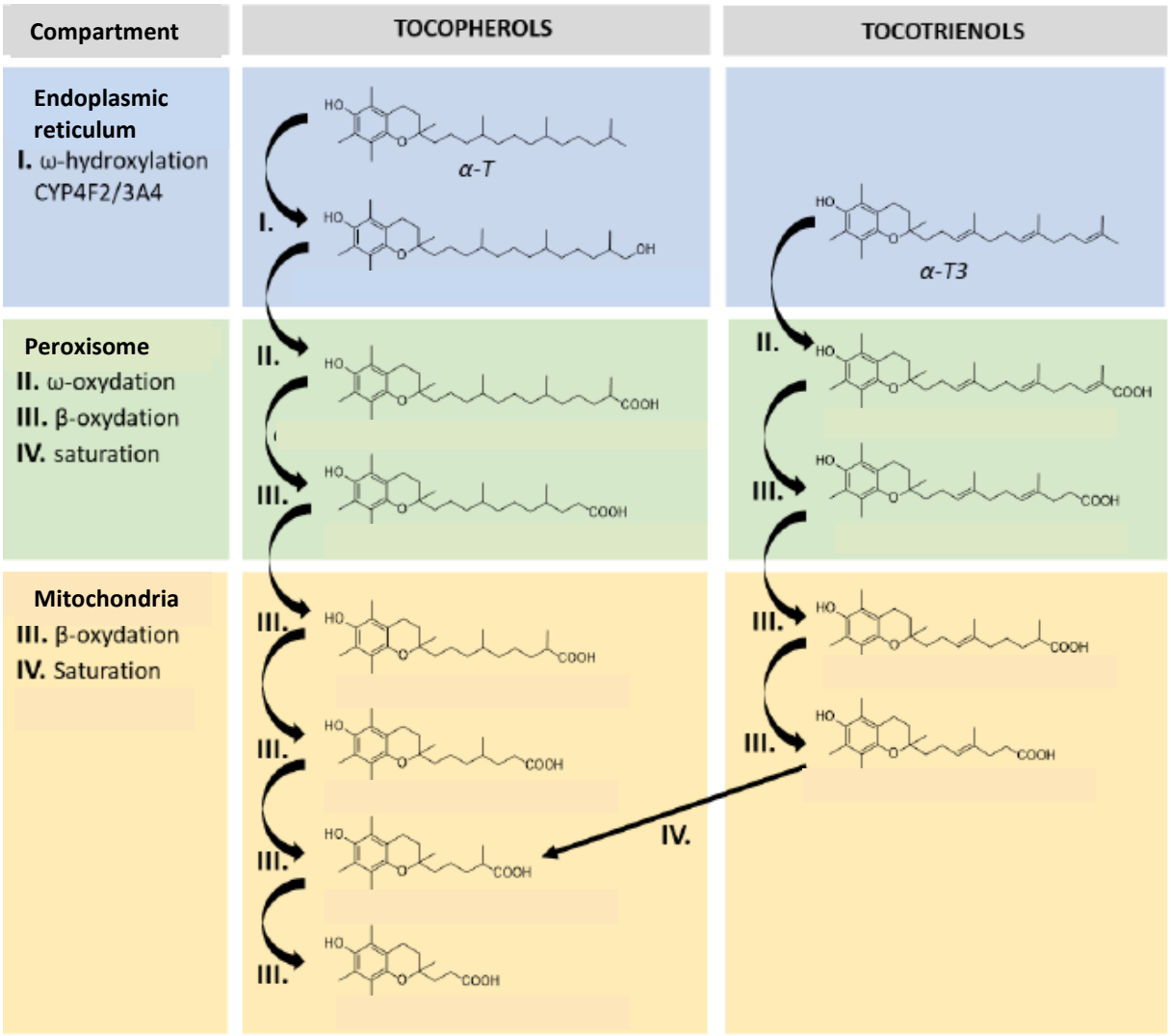

Figure 4: Metabolism of tocopherols and tocotrienols. [13]

1.3 Natural sources of vitamin E

Vitamin E is the main fat-soluble antioxidant in the human and animal tissues. [16] VE derivatives cannot be synthesized by the human body and hence, they need to be provided by the daily diet. [4] The current intake recommendations for vitamin E vary between 3 and 15 mg/day in different countries and depend on the age of the person. [3]

The main dietary sources of VE are found mostly in lipid rich plant products as exemplified by olive, sesame, cotton seed, sunflower oils; edible nuts and nut oil (almond, peanut, walnut, hazelnut); leafy green vegetables; soybeans or wheat germs. [4,10,16-18] We can include also animal products among the sources of vitamin E, but the amount is several times lower, just few examples: egg yolk, sea fish, oysters, butter, cheese, etc. [16,18] For comparison: wheat germ oil contains more than 150 mg/100 g of VE, while oysters only 2 mg/100 g – based on alpha-tocopherol, which is the most common and major homologue found in lipid rich products. [16-18]

Sources of tocotrienols are not significantly widespread; the major sources of them in human nutrition are concentrated in plant aliment such as cereal grains (oat, barley, rye, and annatto) and certain vegetable oils (palm oil, coconut oil, or rice bran oil). [1,16,18,19]

Table 1 The contents of tocopherols and tocotrienols (mg/100 g of oil) in some common edible oils. [1,16,18]

Oil	*α-T*	*β-T*	*γ-T*	*δ-T*	*α-T3*	*β-T3*	*γ-T3*	*δ-T3*
Barley	14.2-20.1	0.6-1.9	3.5-15.1	0.9-4.6	46.5-76.1	nd-12.4	8.5-18.5	0.5-2.6
Coconut	0.2-1.8	tr-0.3	tr-0.1	nd-0.4	1.1-3.0	nd-0.2	0.3-0.6	nd-0.1
cotton seed	30.5-57.3	0.3	10.5-31.7	nr	nr	nr	nr	nr
Olive	11.0-17.0	nd-0.3	0.9-1.3	nd	nd	nd	nd	nd
Palm	6.1-42.0	nd-0.4	nd	nd	5.7-26.0	nr-0.8	11.3-36.0	3.3-8.0
Peanut	8.9-30.4	nd-0.4	3.5-19.2	0.9-3.1	nd	nd	nd	nd
Rice bran	0.7-15.9	0.2-2.5	0.3-8.0	0.1-2.7	0.8-13.8	tr-2.6	1.7-23.1	0.1-2.5
Sesame	0.24-36.0	0.3-0.8	16.0-57.0	0.2-13.0	tr	nd	nd	nd
Soybean	9.5-12.0	1.0-1.3	61.0-69.9	23.9-26.0	nd	nd	nd	nd
Sunflower	32.7-59.0	tr-2.4	1.4-4.5	0.3-0.5	0.1	nd	tr	tr
Wheat germ	151-192	31.2-65.0	32.2-52.3	nd-0.6	2.5-3.6	nd-8.2	nd-1.9	nd-0.2

nd: not detected, nr: not reported; tr: trace

Only a few sources contain enough amounts of tocotrienols to be able to be used for processing in the food, pharmaceutical or cosmetic industry. [1]

1.3.1 *The main sources of tocotrienols and their analogues*

Bixa orellana L.

Bixa Orellana L. is a 3-10 meters in height evergreen tree, which is native to Central and South America (mainly Mexico, Brazil, Ecuador and Peru), nowadays widespread to other tropical parts of the world (India, Indonesia). [20,21] The plant is also known by the name annatto, achiote or roucou and belongs to a small family of *Bixaceae*. [20,22] The most commercial important parts of the plant are red pyramidal shaped seeds found in bivalve capsules. Each capsule contains on average 30-45 seeds. [20] These seeds (especially their pericarps) are frequently used as a red to yellow pigment or a dye for pharmaceutical, textile, cosmetic and particularly food industry (frequent colorant of dairy products – cheeses, margarines). [20-22] Red to yellow colours are mainly provided by the carotenoids (bixin and norbixin). [21,22] This food colorant could be found under acronym E160b. [21] Annatto oil obtained from seeds is very rich for tocotrienols (predominantly γ, δ isomers; α, β isomers only in traces), essential oils (eugenol, eugenyl acetate, β-caryophyllene and α-humulene), and also the above-mentioned carotenoids. [16,23] Geranylgeraniol – a diterpene alcohol is another important compound found in annatto oil. Its extracts were under preliminary research as of 2015 to determine their potential biological properties in humans. In one such application, annatto geranylgeraniol is an ingredient in an experimental medical food being investigated for its effect on blood lipoproteins. [24] It is also a potent inhibitor of *Mycobacterium tuberculosis in vitro.* [25]

Figure 5: *Bixa orellana L.*: The tree and seeds in capsule. [26]

It must be said that *Bixa Orellana L.* has a rich tradition as folkloric remedies in tropical countries of Central and South America. The leaves, their decoctions and extracts have been used to treat headache, fever, various microbial diseases, and indigestion. [22] Seeds have been used as a condiment as well as laxative, antidiabetic, hypotensive, expectorant, and antibiotic. [20]

Palm oil

Palm oil is considered one of the major sources of VE. It contains between 600 and 1000 mg/L of VE. The oil is extracted from the orange mesocarp of the fruit of the oil palm tree (*Elaeis guineensis*). [27,28] The palm tree is an ancient tropical plant native to many West African countries, where local populations traditionally use its oil for cooking and other purposes. Large scale palm crops are found across the tropical regions of the world. Nowadays Malaysia and Indonesia are the leading producers of palm oil, accounting for 86 % of the global production. [28] The refining of crude palm oil (CPO) is a long and tedious process that provides a large number of derived products. CPO contains about 1 % minor components: carotenoids, vitamin E (tocopherols and tocotrienols), sterols, phospholipids, glycolipids, terpenic and aliphatic hydrocarbons. [29] Carotenoids, T and T3 are the most important for their highest amount of these minor components and contribute to stability and properties of palm oil. [29]

The palm oil is used in many branches of industry; it is commonly used in cosmetics and it plays the main role in food processing industry (processed food, bakery). It is also used to produce biofuels. [30,31] That can be used as alternatives to fossil fuels such as diesel. [30] Although palm oil is less suitable than other vegetable oils owing to its high viscosity and lower energy density, it gives high yields at low prices, and hence is likely to be important in meeting biofuel demand. [30,32]

Uncontrolled oil palm fields expansion is a serious threat to biodiversity in South-East Asia, and with recent campaigns against the crop, it is easy to forget that oil palm provides nearly 30 % of the world's edible vegetable oil, and has been a major force for poverty alleviation and rural development in the tropics. [30,32] Forcible tropical deforestation caused mainly by large conglomerates is both a major source of carbon dioxide emissions and a leading cause of many endemic species extinctions (for instance: orangutans, Sumatran tigers and many others). [30] For these social and environmental reasons, palm oil is currently subject to a lot of controversy.

Rice bran oil (RBO)

Rice belongs to a genus of *Oryza* and is classified in the family of *Poaceae*. It is the most generally consumed essential food for the majority of the world's human population, mainly in Asia. [33] The rice bran oil is obtained from the rice husk (the outer hard brown layer of the

rice grains), a by-product of rice milling industry and it is a natural source rich in VE (approximately 300 μg/g). [34] The four major vitamins are α-T/T3 and γ-T/T3. [34,35]

World rice production is greater than 500 million metric tons with India, China, and Japan the leading producers. About 60 million tons of rice bran are obtained each year, as a by-product. Therefore, rice bran is considered the best source of T3 in terms of availability. [34]

Figure 6: Rice grains with husk and completely refined rice grains. [36]

The literature sources show that T3 and its derivatives were presented in plant species belonging to these families: *Pinaceae, Canellaceae, Poaceae,* and *Clusiaceae*. [1] The latter have been subject of several studies of SONAS, who lately focused on plant species of the genus *Garcinia*.

Genus Garcinia L.

Garcinia L. is a tropically distributed angiosperm genus with high species richness in South East Asia, Equatorial Africa and Polynesia. It is composed of more than 240 woody tree species. [37,38] This genus belongs to the family of *Clusiaceae.* [37]

Garcinia kola Heckel

Garcinia kola Heckel is a medium sized tree found in the moist forests and widely distributed throughout West and Central Africa (Cameroon, Senegal, Nigeria, and Ivory Coast). Its edible nuts are known chiefly as “bitter kola”. [39] The plant has been referred to as a “wonder plant” because every part of it has been found to own a medicinal importance. The fruit, leaves and bark of the plant have been used for centuries for treatment of cough, fever, hepatitis, diarrhoea, and gonorrhoea. [40] The seeds are used in folk medicine and in many herbal preparations for

the treatment of ailments such as laryngitis, liver disorders, and bronchitis. [39] The seeds are also employed as a general tonic and they are believed to have aphrodisiac properties. [39,40]

Figure 7: Nuts of *G.kola.* [41]

Because of its wide applications in traditional African medicine, the researchers were quite interested in the metabolites of this plant. Thus, in 1997, Terashima et al. have identified and isolated two new chromanols from a methanolic extract of *G. kola* nut. They were named as δ-garcinoic acid (AG) (0.38% yield) and garcinal (0.0013% yield) and were isolated together with a known product δ-T3 (0,0012% yield) and three also known biflavonoids. [42,43] Garcinoic acid, garcinal and δ-tocotrienol showed about 1,5 times stronger antioxidation activity than α-tocopherol. [42]

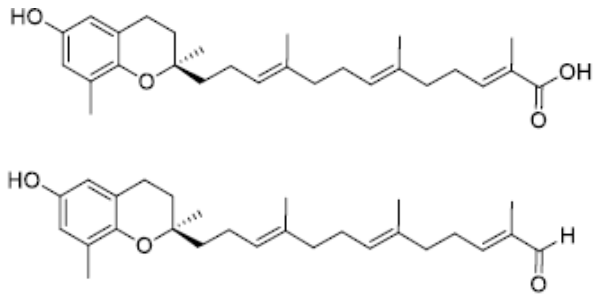

garcinoic acid

garcinal

Figure 8: New oxidized T3 derivatives found by Terashima et al. [42]

Garcinia amplexicaulis

Garcinia amplexicaulis is an endemic shrub 3-4 meters high with yellow blooms from the south of New Caledonia. [44] It is one of the few plants which are hyperaccumulators of manganese – it could be used in the revegetation of the mining site with regard to recovering biomass rich in manganese. [45]

Figure 10: *Garcinia amplexicaulis* shrub. [46]

It is crucial for our study that the barks of *Garcinia amplexicaulis* have high content of two major derivatives of VE: δ- and γ-amplexichromanol (AC). They are obtained from their DCM extracts. The estimated amounts are between 1.5 to 1.8% yield of dry plant for δ-amplexichromanol and about 0.2 to 0.7% yield for γ-amplexichromanol. They were found to be antiangiogenic agents in the low nanomolar range. Amplexichromanols are chromanols with an oxidated terminal prenyl unit (secondary allylic alcohol). Natural occurring tocotrienols-like compounds with two primary alcohol functions located at the terminal part of the farnesyl chain are very unique to this day; therefore, *G. amplexicaulis* was very attractive for further study. Its follow-up deepening studies have proved and described ten utterly new tocotrienol-like compounds, i.e. amplexichromanols; moreover, eleven known compounds were also isolated during this investigation. [44]

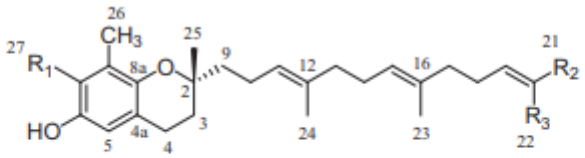

	R_1	R_2	R_3
δ-amplexichromanol	-H	$-CH_2OH$	$-CH_2OH$
γ-amplexichromanol	$-CH_3$	$-CH_2OH$	$-CH_2OH$

Figure 9: Structures of two major secondary metabolites isolated from the barks of *G. amplexicaulis*. [44]

1.4 Biological properties of vitamin E

Tocotrienols and tocopherols have long been only associated with vitamin E, i.e. the main lipid-soluble antioxidant in tissues. However, in the last 20 years, tocotrienols have been reported to possess a wide range of biological activities, including inhibition of cholesterol biosynthesis, antiangiogenic, and proapoptotic effects. [1]

1.4.1 *Antioxidant activity*

The generation of free radicals resulting from the incomplete reduction of molecular oxygen during aerobic respiration is closely related to cellular damage. The regulation of the equilibrium between the production of reactive oxygen species (ROS) by cellular processes and their elimination by the antioxidant defense system keeps the physiological processes at homeostasis. [4] Antioxidant activity of VE has been studied since its discovery in 1922. Tocopherols and tocotrienols intercalate into the cell membrane due to their strong lipophilicity, where they very effectively inhibit lipid peroxidation by scavenging the lipid peroxyl and alkoxyl radicals. [1,5] The hydroxyl group of the aromatic ring of the chromanol "head" can donate hydrogen radical to scavenge lipid peroxyl radicals which halts their propagation in membrane. [19,40] When vitamin E scavenges peroxyl radicals, it is converted into vitamin E radical, which may be further oxidized into tocopheryl quinone or epoxy-tocopheryl quinone or reduced by reducing compounds (such as vitamin C, syn: ascorbate) to regenerate the antioxidant capacity of VE. [4,47] Some of the studies have indicated that α-tocotrienol is a more efficient antioxidant than α-tocopherol because it is recycled more efficiently from its chromanoxyl radical and is more uniformly distributed in the cellular membrane layer. [1]

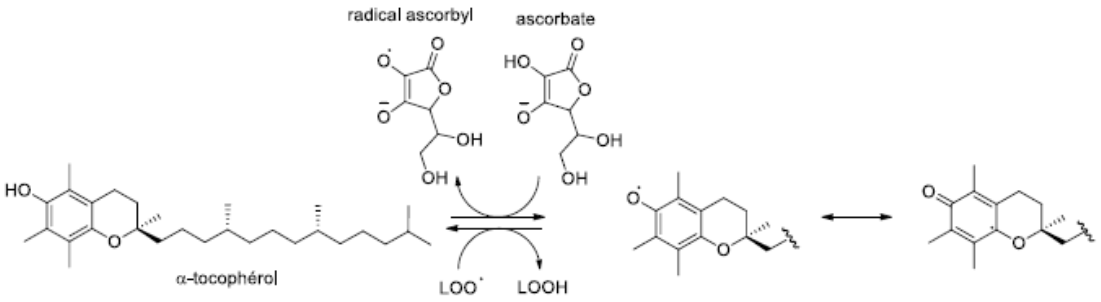

Figure 11: Antioxidant activity of VE. [48]

1.4.2 *Inhibition of cholesterol biosynthesis*

The interest in tocotrienol form of natural VE, not tocopherols, as a hypocholesterolemic compound began when Qureshi *et al.* in 1986 attributed the major cholesterol-lowering action of barley to be at the level of cholesterol synthesis. [19,49,50] By sequential extraction of barley, α-tocotrienol was identified as the chemical constituent responsible for inhibiting the leading enzyme of the cholesterol biosynthetic pathway, 3-hydroxy-3-methyl-glutaryl-coenzyme A reductase (HMG-CoA reductase). [19,49] HMG-CoA reductase produces mevalonate, which is subsequently converted to sterols and other products. It is proposed that tocotrienols are effective in lowering serum total and LDL-cholesterol levels by inhibiting the hepatic enzymatic activity of HMG-CoA reductase through a post-transcriptional down-regulative mechanism in degradation of enzyme, whereas commonly used statins act directly as competitive inhibitors of HMG-CoA reductase. [1,19,49] Interestingly, α-tocopherol had an opposite effect on this enzyme, it significantly induced its activity. This contrast was of outstanding significance and definitely required further characterization. [50]

1.4.3 *Cardioprotective activity*

Cardiovascular diseases (CVD) are multifactorial disease involving both genetic and environmental factors. Although, newer approaches to improve dietary behaviours have significantly reduced the mortality rate, the number of individuals with CVD remains the biggest cause of deaths worldwide up to this time. [4,51]

CVD are diseases that lead to the constant search for new and more effective preventive methods that can reduce the risk of its developing. In the 1990s, the benefits of α-T for preventing CVD have been widely studied. Stephens et al. showed that supplementation with α-T (400 or 800 IU per day) in patients with coronary artery disease resulted in a 77% reduction in the risk of myocardial infarction. [52] After this research, many studies have hypothesized that α-T may prevent the oxidation of low-density lipoprotein (LDL), a process involved in the formation of atherosclerotic plaques. [53,54] However, this theory still remains controversial as some studies have failed to demonstrate a significant association between plasma LDL-cholesterol levels and decreased mortality from cardiovascular diseases. [55,56]

Later, other biological studies have been developed to explore the relationship between T3 and CVD. Tocotrienols' cardioprotective effects are mediated mostly through their antioxidant mechanisms and their ability to suppress inflammation (see below), to also inhibit HMG-CoA

reductase, and to reduce the expression of adhesion molecules and monocyte-endothelial cell adhesion. [4,51,57] According to the antioxidant effect of T3, other researchers have shown that supplementation with T3 also reduces lipid peroxide levels in the blood with apparent improvement in blood flow for patients with atherosclerosis. [58]

1.4.4 *Anticancerogenic effect*

One of the first studies addressing the role of VE, specifically tocotrienols, in neoplastic disorders, was reported in 1989. [17] The effects of intraperitoneally injected α- and γ-tocotrienol to mice, as well as that of α-tocopherol, have been examined. Both tocotrienols were effective against sarcoma 180, Ehrlich carcinoma, and invasive mammary carcinoma. [17,59,60] In another independent study published in the same year, the anticarcinogenic properties of palm oil, a rich source of tocotrienols, was reported. [17] Subsequently, numerous investigations have evinced the anti-cancer potential of T3 in cancers of the breast, colorectal, liver, lung, pancreas, prostate, stomach etc. [59] Unlike in the case of neuroprotection (mentioned below) where α-tocotrienol has emerged to be the most potent isoform, it has been reported that γ- and δ-tocotrienols are the most potent anti-cancer isoforms of all natural existing tocotrienols. [4,50,60] In contrast to tocotrienols, α-tocopherol is not as effective. It was discovered that the antioxidant or redox effect of tocotrienols is not responsible for its anti-cancer property. [17,60] The mode of anti-cancer action could be briefly explained as: a) Tocotrienols exert anti-cancer activity on tumour cells by cell cycle arrest through the induction of cell cycle inhibitors protein and decreased expression of cyclin dependent kinase. b) They also work as an anticancer agent by inhibiting angiogenesis or by enhancing immunity and inhibition of tumour cell migration. c) In human pancreatic cancer cells tocotrienols induce cell-cycle arrest and mitochondria mediated apoptosis. [4, 17, 50,59]

1.4.5 *Neuroprotective effect*

While γ and δ-tocotrienol have been demonstrated to induce specific responses in cancer cells with little or no effects on normal cells, α-tocotrienol has been frequently reported to exert protective activity on normal neuronal cells and, in general, on central nervous system. [50,61] It was suggested that tocotrienols may have protected cells by an antioxidant-independent mechanism. Examination of signal transduction pathways revealed that protein tyrosine phosphorylation processes played a central role in the execution of death. [4]

A specific research conducted by Sen et al. (2007) led to the first evidence that α-tocotrienol is the most potent neuroprotective isoform of VE in glutamate-induced degeneration of HT4 hippocampal neurons and its strong protective effects against neurodegeneration. Originally, the authors described the potentiality of nanomolar concentrations of α-tocotrienol, (not α-tocopherol) to obstruct glutamate-induced cell death. [50,61] Glutamate is one of the most important neurotransmitters; but, at high concentrations, it induces a rise of intracellular Ca^{2+} and mitochondrial dysfunction. α-tocotrienol inhibits cell death by concealing the activation of c-Src kinase (proto-oncogene tyrosine-protein kinase Src) and ERK (extracellular signal–regulated kinases) phosphorylation in HT4 hippocampal neurons. [50] Very surprisingly, the concentrations used in this study were 4–10-fold lower than levels detected in plasma of supplemented humans, indicating that α-tocotrienol regulates a specific signal transduction pathway insensitive to comparable concentrations of tocopherol. It clearly suggests that this activity is completely independent of its antioxidant capacity. [17,50,61]

The neuroprotective activity tocotrienols and, particularly, of α-tocotrienol, has been also confirmed by Osakada et al. (2004). In their research, they observed that VE mixture from palm oil (further purified in order to eliminate α-tocopherol), pure α-, γ- and δ-tocotrienol (0,1-10 μM) significantly protects primary neuronal cells from rat striatum challenged by different pro-oxidants. They utilized, to be specific, hydrogen peroxide, a superoxide generating molecule (paraquat), nitric oxide donors (S-nitrosocysteine and 3-morpholinosydnonimine) and an inhibitor of glutathione synthesis L-buthionine-[S,R]-sulfoximine. Contrarily, α-tocopherol was ineffective in all cases of the study, which testifies the proof of a specific tocotrienol activity unrelated to their nucleophilic, antioxidant, properties. [17,61,62]

1.4.6 *Anti-inflammatory effect*

Inflammation results from overreacting immune response and is characterized by the production of a multitude of reactive oxygen/nitrogen species and proinflammatory mediators, including lipid mediators, notably prostaglandins and leukotrienes, and cytokines such as TNF-α and interleukin-6 (IL-6), which in turn aggravate inflammation and lead to excessive damage to host tissues (described in details below). [4,5,63]

The anti-inflammatory potential of dietary T and T3 is well known. The study conducted by Reddanna *et al.* (1990) showed inhibition of 5-LOX purified by α-T (IC_{50} = 5 μM). [64] Similarly, Jiang *et al.* studied the effect of VE derivatives on COX-2 catalyzed PGE2 synthesis in human pulmonary epithelial A549 cells. IC_{50} values were above 50 μM for α-T and between

1 and 3 μM for δ-T and γ-T3. The mechanistic studies of Jiang *et al.* demonstrated the anti-inflammatory effect of γ-T, δ-T and T3 by inhibition of COXs and 5-LOX. [65,66] Recently, Jiang has demonstrated the anti-inflammatory effect of δ-garcinoic acid on the COX-1/2 and 5-LOX targets. In fact, it inhibits 50 % of the activity of 5-LOX and COX-2 at concentrations of 1,0 μM and 9,8 μM, respectively. [66] Long-chain carboxychromanols, especially 13'-COOHs, have been shown to inhibit COXs and 5-LOX more strongly than unmetabolized vitamin E forms. [5]

The latest study conducted by Pein et al. (2018) proves that long-chain ω-carboxylates are potent allosteric inhibitors of 5-LOX, a key enzyme in the biosynthesis of chemoattractant and vasoactive leukotrienes. During their study they made the library screening of potential human vitamin E metabolites. Firstly, the library was based on an original set of ω-oxidized T3 isolated from *Garcinia amplexicaulis* (*Clusiaceae*). Next, semisynthesized analogues were also evaluated corresponding to intermediates of human vitamin E metabolism. Screening of this library for inhibition of 5-LOX revealed high-affinity inhibitors among ω-alcohols and ω-carboxylates, including T and TE metabolites of the α-, β-, γ-, and δ-series, with the ω-carboxylated δ-T3 (δ-T3-13′-COOH = δ-garcinoic acid) being most potent (IC_{50} = 35 nM). Metabolites with truncated side chain (5′- and 3′- carboxyethyl hydroxychromanols, produced by repeated cycles of β-oxidation) markedly lost 5-LOX inhibitory activity (IC_{50} > 3 μM). Moreover, all this library provided mechanistic insights into the binding mode and inhibitory mechanism of 5-LOX thereby confirming the novel allosteric mode of enzyme inhibition. [67]

2 Inflammation

Inflammation is a word taken from the Latin word "*inflammare*" which means "to burn". It is an important and necessary immune system's defensive process of the human body. [64] It is generally defined as a response to stimulation by invading pathogens, toxic compounds, irradiation, or endogenous signals such as damaged cells that results in tissue repair or sometimes pathology, when the response goes unchecked. [64,68,69] The result is the mobilization of various circulating cell lines (neutrophils, monocytes, macrophages ...) or tissue resident (macrophages, mast cells, fibroblasts ...), and chemical mediators such as cytokines, vasoactive amines or eicosanoids. [70-72] The body attempts to start the healing process following an assault, to defend against foreign bodies, such as viruses and bacteria, and to repair damaged tissue. [68,73] The manifestations of inflammation have been known since antiquity: "*rubor*" redness, "*calor*" heat, "*tumor*" swelling, "*dolor*" pain and "*functio laesa*" loss of function. [63,69]

When badly controlled inflammation progresses from acute to chronic. Chronic inflammation significantly contributes to the development of chronic diseases including cardiovascular diseases, neurodegenerative diseases and cancer. [4,5,73] Chronic inflammatory diseases such as rheumatoid arthritis and asthma are among the leading causes of disability worldwide. [68,73]

2.1 Arachidonic acid metabolism

Arachidonic acid (AA, C20:4 ω-6) is a polyunsaturated fatty acids with 20 carbon atoms present in the phospholipids of membranes of the body's cells. AA is a lipid mediator generated from cell membrane lipids by the catalysis of phospholipase A2, which is further oxidized by cyclooxygenase (COX) and lipoxygenase (LOX) enzymes to produce a group of proinflammatory mediators called eicosanoids. [68]

The COX pathway leads to the prostanoids. For instance it produces vasodilator prostaglandins such as PGE2 and prostacyclin (PGI2) and also thromboxane A4, a potent platelet aggregating agent. [70,74] The LOX pathways leads to the leukotrienes (LT). Leukotrienes are formed by initial oxygenation at C-5 followed by further transformation to an unstable epoxide intermediate, leukotriene A4 (LTA4). This intermediate can be converted into LTB4 by hydrolysis and into LTC4 by conjugation with glutathione. [74]

Generally, eicosanoids play an essential role in the inflammatory response and present in all organs and tissues where they exert a regulating function and a mediating role in the activity of cells during many processes. They are produced following a cellular stimulation, e. g. infection, blow, wound, burn, allergy etc. However, their chronic presence can aggravate the inflammation and lead to significant damage in host tissues. [72]

For instance, prostaglandin E2 (PGE2) produced from COX-1 and COX-2 is believed to cause pain and fever, as well as activating cytokine formation. [5] LTB4, a lipid mediator originated from the 5-LOX-catalyzed reaction in neutrophils, is one of the most potent chemotactic agents. [70] LT C4 and D4, which are also generated by 5-LOX in eosinophils and mast cells, play key roles in allergic inflammatory diseases and asthma. [5] COX- and 5-LOX-catalyzed eicosanoids are known to promote different types of cancer. Because of the central roles of PGE2 and LTB4 in inflammation, COX and 5-LOX have been recognized as key targets for drug therapy against chronic inflammation diseases. In particular, COX inhibitors, which are nonsteroidal anti-inflammatory drugs (NSAIDs), have proven efficacy in attenuating inflammatory response, and treating inflammatory diseases. The 5-LOX inhibitor zileuton has clinically been used to treat asthma. [5,70,72]

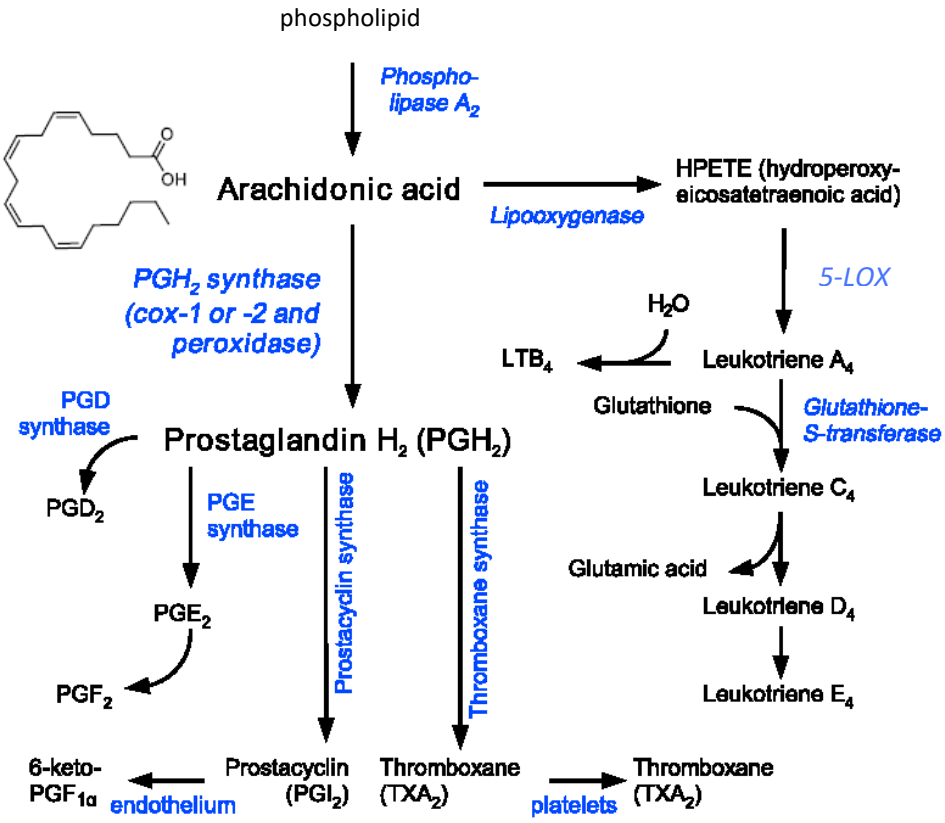

Figure 12: Basic scheme of arachidonic acid pathway. [70,71,74]

2.1.1 *Cyclooxygenase pathway*

COX was characterized in 1967 for the first time and quite a few years later 2 isoforms of COX were reported. [75,76] COX enzymes (also called as prostaglandin endoperoxide H synthases – PGHS) catalyze the committed step in prostaglandin synthesis – the conversion of arachidonic acid (AA) to prostaglandin H2 (PGH2), the common biosynthetic precursor to prostaglandins and thromboxane. [77,78]

COX-1 is constitutively expressed in most tissues and is required for the production of PGs involved in basic housekeeping functions throughout the body. COX-2 is primarily an inducible enzyme (constitutively expressed in certain tissues, for example, brain and kidney), whose expression is activated in a variety of cells in response to cytokines, mitogens, endotoxins and tumour promoters in different types of cells. [72,77]

COX-1 and COX-2 exist as homodimers with a molecular mass of approximately 70 kDa per monomer. They are composed of 576 and 581 amino acids, respectively. The COXs share a high degree of amino acid sequence identity (~60%) and structural homology. Their tertiary and quaternary structures are virtually identical. [77,78] Each subunit of the dimer contains the active sites of COX and peroxidase. Thus, both isoenzymes share the same activities and catalyze the biosynthesis of prostaglandins. The COXs are located on the luminal surface of the endoplasmic reticulum as well as on the internal and external membranes of the nuclear envelope. [70,77,78]

Despite of their structural similarity, COX-1 and COX-2 differ substantially in their regulation of protein expression and the roles in tissue biology and diseases. [70]

COXs inhibitors

The COXs enzymes are very popular targets for treatment of inflammatory diseases. After that year, the exponential development of non-steroidal anti-inflammatory drugs (NSAIDs) has begun. [75] NSAIDs block the COX-1 and COX-2 isoenzymes, leading to a decrease in proinflammatory metabolites such as PGE_2. NSAIDs also reduce aches and pain. They are used in the treatment of various diseases with an inflammatory component such as atopic dermatitis or rheumatoid arthritis. [76-78] The first COX inhibitor was acetylsalicylic acid. The development of new NSAID drugs was based on this derivative. Thus, there are several

subgroups among the family of NSAIDs such as acetic acid derivatives, propionic acid derivatives, enolic acid (oxicams) etc.

The group of acetic acid NSAIDs corresponds to the compounds in which a CH_2 link is interposed between the acid group and the cyclic unit. Indomethacin with an indole structure is the leader in this group. For propionic acid NSAIDs, they can be considered as homologs of acetic acid drugs. In this group we find ibuprofen, ketoprofen, naproxen etc. Enolic acid derivatives or oxicams are another major category. They are characterized by a heterocyclic sulfur and nitrogen system. Unlike conventional NSAIDs, the compounds are devoid of a carboxylic group.

Finally, there should be mentioned paracetamol (acetaminophen), the most prescribed molecule in the world. Actually, it is not considered as NSAID because it has little anti-inflammatory activity. It treats pain mainly by blocking COX-2, mostly in the central nervous system, but not much in the rest of the body. Despite the huge collection of scientific data and the existence of a perfectly effective antidote, nowadays, paracetamol still remains the leading cause of acute liver failure in Western world and one of the causes of death by intoxication. [79]

The mechanism of action of NSAIDs and their side effects were understood during the discovery of COX-2. Available scientific evidence suggests that the anti-inflammatory and analgesic properties of traditional NSAIDs are due to inhibition of COX-2, whereas the gastrointestinal side effects of these inhibitors are associated with inhibition of COX-1. [76,77] Therefore, the administration of NSAIDs, to treat chronic inflammatory diseases such as osteoarthritis or rheumatoid arthritis, inevitably leads to a lack of PG required for certain physiological functions.

The long-term use of NSAIDs often causes gastrointestinal problems (irritations or ulcers). (80) It may also promote the development of kidney problems and hypertension. [81,82] In 1990s, a certain hypothesis was advanced that these side effects could be prevented by selective COX-2 inhibition. [75] In 1999, the family of coxibs was introduced as selective inhibitors of COX-2. Coxibs share the beneficial anti-inflammatory, antipyretic and analgesic properties of traditional NSAIDs, but do not have the associated severe gastric toxicity. [75,82,83] In 2004, Merck and Company withdrew rofecoxib, a COX-2 selective inhibitor due to severe cardiovascular side effects (arterial hypertension, myocardial infarction, stroke, and heart

failure), followed by withdrawal of most other coxibs. Only celecoxib and etoricoxib are currently marketed. [77,84]

2.1.2 *Lipoxygenase pathway*

The lipoxygenase pathway in human beings mainly consists of three enzymes, 5-, 12- and 15-LOX, they catalyze the insertion of one molecular oxygen into the 5-, 12- or 15- carbon position of AA and are termed 5-LOX, 12-LOX and 15-LOX, accordingly. The primary products are 5S-, 12S-, or S-hydroperoxyeicosatetraenoic acid (5-, 12-, or 15- HPETE), which can be further reduced by glutathione peroxidase to the hydroxy forms (5-, 8-, 12-, 15-HETE), respectively. [70,76] The concomitant action of 5-LOX and 12- or 15-LOX is responsible for the synthesis of lipoxins (LXs), which are involved in resolution of inflammation. The 5-LOX, the key enzyme of this pathway, is a dioxygenase that catalyses two steps in the biosynthesis of leukotrienes, assisted by the cofactors Ca^{2+} and ATP, along with protein–protein interactions involving 5-LOX activating protein (FLAP). In contrast to 12- and 15-LOX, 5-LOX catalyses a second oxidation step leading to the formation of the epoxy-leukotriene LTA_4 from 5-HPETE. [76]

Lipoxygenases (LOX) have been highly implicated in asthma, allergic rhinitis, osteoarthritis, immune disorders, and various cancers, LTs play a minor role in the pathophysiology of inflammatory bowel diseases and psoriasis in humans. [70,85,86]

Although, the discovery of 5-lipoxygenase dates back to 1976, the exact 3D structure of human 5-LOX was published by Gilbert et al. in 2011. 5-LOX has a molecular weight of 78 kD and contains 673 amino acids and Fe^{2+} ion that plays an important role in AA metabolism. It has

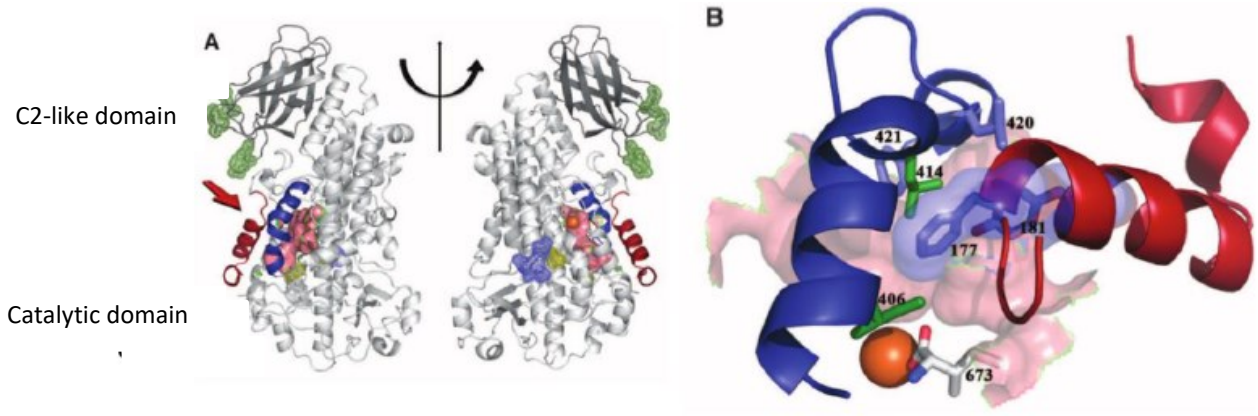

Figure 13: (A) 3D structure of the 5-LOX; (B) Coordination of Fe^{2+} (orange bead) in the active site of 5-LOX according to Gilbert et al. [86]

two domains: N-terminal C2-like domain (about 120 amino acids, mainly composed of β-sheets) and the larger C-terminal catalytic domain which is mainly helical in structure. [85,86]

The catalytic domain contains a non-heme iron ion that acts as an acceptor or donor of electrons. The iron of the inactive 5-LOX is ferrous (Fe^{2+}), and the enzyme requires conversion to the ferric form (Fe^{3+}) to begin the catalytic cycle. Oxidation of Fe^{2+} to Fe^{3+} is provided at the active site by various lipid hydroperoxides. The "C2-like" domain has a regulatory function. It binds to various lipids (phosphatidylcholine, diacylglycerides, etc.), as well as ions such as Ca^{2+} or Mg^{2+}. [85,87]

5-LOX is primarily expressed in various leukocytes: polymorphonuclear leukocytes (neutrophils and eosinophils); monocytes and macrophages; dendritic cells; mast cells; B-lymphocytes; and in foam cells of human atherosclerotic tissue. [85]

LOXs inhibitors

Drugs targeting the LOX pathway can interact at different stages: direct 5-LOX inhibition, FLAP-inhibition, LTA_4 hydrolase inhibition as well as LT receptor antagonism (exemplified by well-known drug montelukast). 5-LOX inhibitors have been developed for over 25 years, but the only drug which entered the US and Canada market yet is zileuton (IC_{50} = 0,5 – 1 μM in stimulated leukocytes), an orally-active drug used for the treatment of asthma with restrictions due to its liver toxicity and a short half-life.[77] Zileuton belongs to class of **(a) iron ligand 5 –LOX inhibitors** which chelate the active site iron via a hydroxyamic acid or N-hydroxyurea moiety. [86]

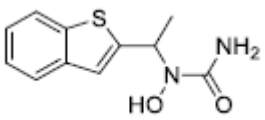

Figure 14: Chemical structure of zileuton. [76]

(b) Redox-active 5-LOX inhibitors comprise lipophilic reduction agents. Among those there are many prominent plant-derived classes like flavonoids, coumarins, quinones, triterpens and other polyphenols. [69,86] Natural or plant-derived substances were among the first 5-LOX inhibitors identified in the early 1980s. To date, a huge number of diverse plant-derived compounds have been reported to interfere with 5-LOX product synthesis. [69] However, many investigations have addressed the efficacy of a given compounds solely in cellular test systems.

Most of them lack suitable oral bioavailability, possess only poor selectivity for 5-LOX and thus, exert strong side-effects due to interference with other biological redox systems or by the production of reactive radical species. [86]

Table 2: Several examples of natural redox-active inhibitors of 5-LOX. [70,86]

	Name	Structure	IC_{50}, cell-free	Plant
Flavonoids	quercetin	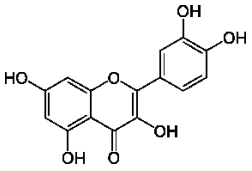	0,3 - 25 µM	*Lonicera japonica*
	cirsiliol	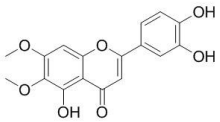	0,1 µM	*Salvia officinalis*
Coumarins	psoralidin	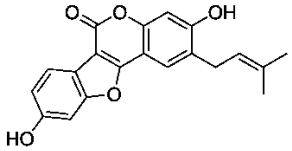	3,6 - 8,8 µM	*Psoralea corylifolia*
Quinones	aethiopinone	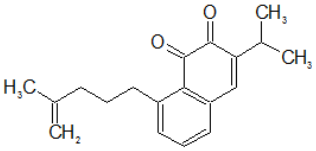	0,11 µM	*Salvia aethiopsis*
Triterpens	3-oxo-tirucallic acid	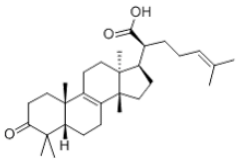	3 µM	*Boswelia serrata*
Polyphenols	Caffeic acid	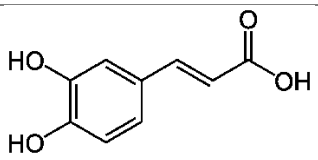	3,7 µM	*Artemisia rubripes*

(c) Non-redox-type 5-LOX inhibitors compete with AA for binding to 5-LOX without redox properties and encompass structurally diverse molecules. It is still unclear if the binding-site of these compounds is in fact the AA substrate-binding cleft in the active site. Thus, experimental data from molecular and biochemical studies suggest an allosteric mode of action for certain inhibitors. [86]

In 2018, Pein et al. reported that LCMs (long-chain metabolites produced by hepatic ω- and β-oxidation of vitamin E) are allosteric 5-LOX inhibitors. This class of 5-LOX inhibitors act at

the C2-like domain, thereby preventing 5-LOX translocation and binding to the nuclear membrane. They showed this phenomenon for δ-T3-13′-COOH (δ-GA) as representative, LCMs inhibit 5-LOX independent of the AA concentration. Their data suggest that δ-T3-13′-COOH (δ-GA) targets a so far unexploited cavity that might represent a potential allosteric binding site for non-competitive 5-LOX inhibitors. [67]

This work has definitely opened “the door” to other investigators and researchers dealing with new possibilities for lipoxygenase inhibition and dealing with new options for the treatment of inflammation.

IV. Experimental part

1 Chemicals

1,4-dioxane, anhydrous, 99.8%, Sigma-Aldrich, USA

2-methylene-1,3-propanediol, 97%, Sigma-Aldrich, USA

4-pentenoic acid, 99%, Fisher Scientific, USA

Acetic anhydride, 99%, Fisher Scientific, USA

Acetone, ≥99.5%, Honeywell, USA

Acetonitrile, for HPLC, for UV, ≥99.9%, Honeywell, USA

Celite ® 545, Fisher Scientific, USA

Crude extract of *Bixa orellana*, CICY, Mexico

Cyclohexane, ≥99%, Honeywell, USA

Deuterated chloroform, ≥99.8 atom % D, Sigma-Aldrich, USA

Dichloromethane, ≥99%, Honeywell, USA

Diethyl ether, ≥99.8%, Honeywell, USA

Distilled water, SONAS, France

Ethanol, 98%, Honeywell, USA

Ethyl acetate, ≥99.5%, Honeywell, USA

Formic acid, ≥95%, Honeywell, USA

Hg-1, Hoveyda-Grubbs Catalyst® 2nd Generation, 97%, Sigma-Aldrich, USA

Hg-2, Grubbs Catalyst® C711, Sigma-Aldrich, USA

Hydrochloric acid, 37%, Sigma-Aldrich, USA

Isopropyl alcohol, ≥98%, Sigma-Aldrich, USA

Lithium hydroxide, 98%, Honeywell, USA

Methanol, ≥99.8%, Sigma Aldrich, USA

Methanol, for HPLC, ≥99.9%, Honeywell, USA

Methyl acrylate, 99%, Fisher Scientific, USA

Methyl methacrylate, 99%, Fisher Scientific, USA

Milli-Q water, SONAS, France

N,N-dimethylformamide, anhydrous, 99.8%, Sigma-Aldrich, USA

N,N,N′,N′-tetramethylethylenediamine, 99%, Fisher Scientific, USA

Oxalyl chloride, 98%, Sigma-Aldrich, USA

Paraformaldehyde, 95%, Sigma-Aldrich, USA

Petroleum ether, ≥ 90%, Honeywell, USA

Potassium hydroxide, flakes, 97%, Honeywell, USA

Potassium permanganate, 99%, Fisher Science, USA

Pyridine, ≥99.0%, Honeywell, USA

Ru-2, Grubbs Catalyst® 2nd Generation, Sigma-Aldrich, USA

Sodium cyanoborohydride, 95%, Sigma-Aldrich, USA

Sodium chloride, >97.0%, SuperU, France

Sodium sulfate anhydrous, ≥99%, Honeywell, USA

Tetrahydrofuran, ≥99.0%, Honeywell, USA

Tosyl chloride, ≥98%, Sigma-Aldrich, USA

Triethylamine, ≥99%, Sigma-Aldrich, USA

2 Materials and methods

All solvents were dried and distilled before usage. Reactions were done under inert atmosphere (N_2). Unless otherwise noted, materials obtained from commercial suppliers were used without further purification. ^{1}H NMR, ^{13}C NMR were recorded on a JEOL 400 MHz spectrometer in deuterated chloroform and calibrated using the residual undeuterated solvent resonance as internal reference. Chemical shifts δ are given in ppm, and coupling constants *J* are given in Hz. IR spectra were recorded on a Thermo Scientific Nicolet iS5 FT-IR Spectrometer and are reported in terms of frequency of absorption (cm^{-1}). TLC were performed on aluminium plates coated with silica gel (Alugram® Xtra Sil G / UV Finished Plates, Germany). The spots are revealed under UV light at 254 and 365 nm, and either by immersion in a solution of potassium permanganate or in CAM (Cerium Ammonium Molybdenum stain). Preparative TLC were used on plates CCM Alugram® Xtra Sil G / UV 254, MACHEREY-NAGEL®, Germany. Column chromatography was performed using silica gel 60Å (particle size 40-63 μm) purchased from Fisher Scientific. Flash chromatography purifications using pre-packed columns (silica, 4 g to 330 g) were realized on a CombiFlash Rf-200 equipped with a gradient pump, a column station with a DASi introduction system, a multi-wavelength UV detector, a fraction collector and a software to control the device. HPLC analyses were performed with a Waters Alliance HPLC system (Milford, CT, USA) equipped with a quaternary HPLC pump, degasser, autosampler, and UV detector (Milford, CT, USA) and column Omnispher C18 (Varian) 250 × 21,4 mm (10 μm). Reactions under microwave irradiation were performed in the Monowave 300 (Anton Paar), equipped with the MAS 24 Autosampler, using borosilicate glass vials with snap caps.

3 Purification of crude extract of *Bixa orellana*

Prepared crude extract of *Bixa orellana* (annatto) made of seeds, a starting material of my work, was obtained through collaboration with researchers from CICY (Centro de Investigación Científica de Yucatán), Mérida, Mexico. The extract had a strong ability to orange-red stain due to carotenoids contained; thus, it was necessary to handle it carefully.

First, a specific amount of crude extract was dissolved in minimum volume of dichloromethane (DCM), silica was added in ratio 1:2, and then the solvent was evaporated by stirring to yield a completely dry powder. Afterwards, it was used for purification by automated flash chromatography.

Flash chromatography is basically an air pressure driven hybrid of medium pressure and short column chromatography which has been optimized for particularly rapid separations. Resolution is measured in terms of the ratio of retention time to peak width. [88] This results in a controlled purification or identification of unknown compounds from organic syntheses, natural product extracts, or other mixtures. During the purification of annatto extract, the column was eluted with cyclohexane (solvent A) and cyclohexane/ethylacetate (7:2) (solvent B) and flow 120 ml/min was used. The polarity of the solvent system increased to 75% cyclohexane/ethylacetate (7:2). The collected fractions were analyzed with silica gel TLC plates using petroleum ether (PE)/acetone/DCM (7:2:1) as a mobile phase. Compounds were visualised under UV light at the wavelength 254 and 365 nm and after visualized by potassium permanganate stain. Similar fractions were pooled together to yield 4 major fractions. They were evaporated under reduced pressure and their purity was verified by ^{1}H NMR spectrometry. Fraction n.1 contained pure γ-T3 (3% yield) and fraction n.3 contained pure δ-T3 (9% yield). These pure compounds were used for further experiments. Other two fractions were not used anymore because of large amount of impurities.

4 Protection of δ-T3

Before the metathesis reaction, it was necessary to protect sensitive phenol function in position C6 of the chromanol ring. In previous studies, it was observed that free phenol function could disrupt the semisynthesis strategy due to its greater reactivity. We firstly chose a tosyl group as the protecting group. Indeed, it is proved to be chemically stable and easy to form with this family of derivatives.

The protection of the phenol of δ-T3 with a tosyl group using triethylamine and 4-toluenesulfonyl chloride was carried out in DCM under nitrogen atmosphere at least 4 hours at room temperature. In particular, the protection conditions have been optimized in order to selectively achieve the protection of phenol.

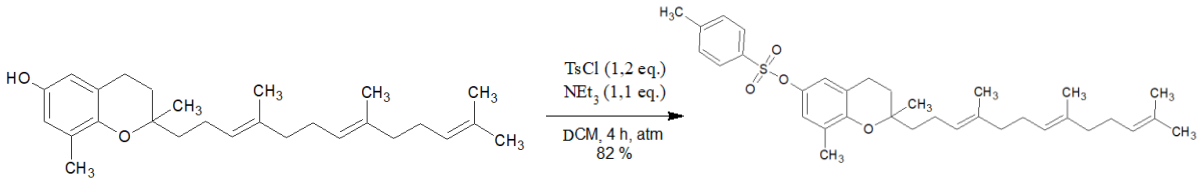

Figure 15: Synthesis of the tosylated δ-T3. [89]

The completion of reaction was confirmed by TLC. The work-up consisted 3 times extraction with diethyl ether, the pooled organic layers were washed twice with water and once with brine. It was dried over anhydrous sodium sulphate, filtered and the solvent was evaporated under reduced pressure. A light brown oil was obtained.

The crude product was purified by automated flash chromatography on silica gel eluted with a mixture of PE/acetone (9:1) (flow 23 ml/min). The polarity of the solvent system increased to 90% PE/Ac (9:1). The collected fractions were analysed by TLC using PE/acetone/DCM (8:1:1) as a mobile phase. The plates were visualised under UV light at 254 and 365 nm and late by $KMnO_4$ stain. The major fraction was evaporated under reduced pressure and its purity was verified by ^1H NMR spectrometry. 82% yield of pure tosylated δ-T3 (TsOδT3) was obtained.

5 Metathesis reaction

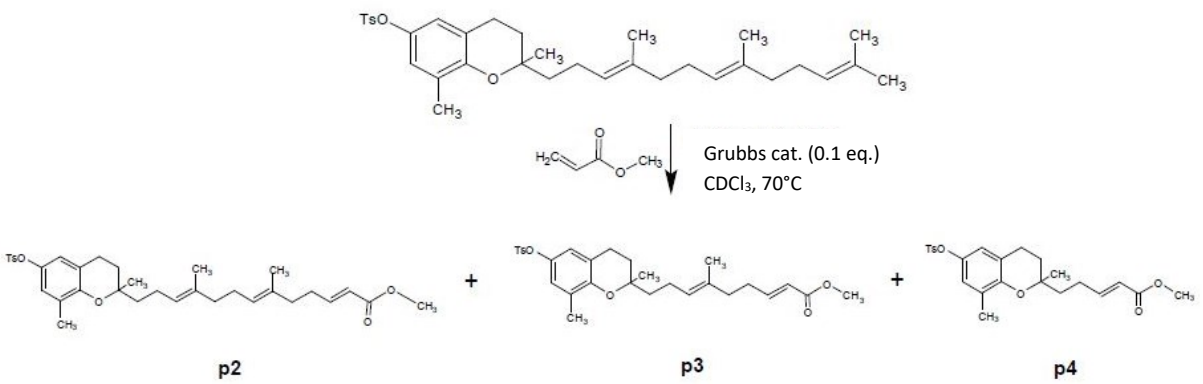

Figure 16: Metathesis reaction. [89]

Optimizing the metathesis reaction to access new T3 derivatives was the main aim of my work. The reaction could be described as cross olefin metathesis (more information in chapter IV.3.3.1). Tosylated δ-T3 reacted with methacrylate (MA) to lead to three major methyl esters. Three compounds are formed because the metathesis takes place on all of three double bonds at carbons 3′, 7′, and 11′ from the farnesyl side chain. The reaction works only with specific catalysts system (described in chapter IV.3.3.1.2).

Time of reaction, type of Grubbs catalysts and equivalence of reactant were the variables during the optimization and they are summarized in Table 3.

Table 3: Variables of the reaction. [89]

Variables of the reaction		
Time	Grubbs catalyst	Equivalence of methacrylate
1 (only for 2.4 eq.), 3, 5, 7 days	Ru-2, Hg-1, Hg-2 (Figure 19)	0.6; 0.8; 1.2; 2.4

The reaction was conducted in a same way every time. Under nitrogen atmosphere, to a solution of TsOδT3 **(30 mg, 0.05 mmol, 1 equiv.)**[2] in degassed deuterated chloroform **(0.7 mL)** were added methylacrylate and Grubbs catalyst **(0.005 mmol, 0.1 equiv.)**. The reaction mixture was bubbled several minutes with nitrogen, the flask with reaction mixture was properly sealed and stirred at **70°C** for 1, 3, 5, 7 days. After determined duration, a sample of reaction mixture was

[2] The conditions in bold have never changed during the optimization.

taken for HPLC analysis (Chapter IV.3.3.2). Then, when the reaction was terminated, the filtration through celite (diatomaceous earth) was carried out, the celite was washed few times with ethyl acetate and the solvent was removed under reduced pressure. Usually the residues of reaction with 0.6 and 0.8 equiv. of methacrylate were purified by preparative TLC on silica gel with a cyclohexane/ethyl acetate mixture 7:2 as a mobile phase to afford the desired products as oil. The spots were detected under UV light, circled and scratched, then the fractions were stirred few minutes in 5 ml of acetone, filtered and washed once with 10 ml of acetone, twice with 10 ml of DCM/methanol mixture (9:1) and again once with 10 ml of acetone. The solvents were removed under reduced pressure to afford the desired products as oil. Identification and purity of fractions were determined by ^{1}H NMR analysis.

The reaction mixtures which were not separated and purified by preparative TLC were pooled together and purified by column chromatography with a mixture of cyclohexane/ethyl acetate (7:2) as the mobile phase.

During my work, together 42.7 mg of p2, 70.0 mg of p3 and 86.3 mg of p4 were obtained as pure products. Subsequently, these products were deprotected (chapter IV.5). All products were analyzed by ^{1}H NMR spectroscopy.

5.1 Olefin methatesis

Olefin metathesis, a kind of organic synthesis where carbon compounds from very simple and small molecular weight to very large, complex polymers; macromolecules and even natural products are synthesized, has become an indispensable method for the formation of carbon–carbon double bonds, finding use in synthetic organic, biological, and materials chemistry. [90,91] Among the many types of transition-metal-catalysed C–C bond forming reactions, it is without a doubt one of the most thriving fields in modern organic synthetic chemistry. This is due to a wide range of transformations that are possible by olefin metathesis with commercially available and user friendly catalysts. [92] In 2005, Nobel Prize in Chemistry has been awarded to the French Yves Chauvin and Americans Richard Schrock and Robert Grubbs for their contribution to metathesis. Chauvin proposed a new mechanism of metathesis, whereas Shrock and Grubbs developed new catalysts for metathesis. [90]

Metathesis of olefins is the thermodynamically controlled reaction in which the molecules are formally fragmented at their double bonds and new olefin molecules result by recombination of fragment originating from different molecules (Figure 17). Metathesis reactions are generally reversible. [90]

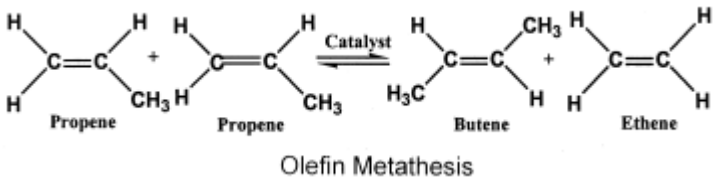

Figure 17: Olefin metathesis. [90]

The Chauvin mechanism involves the [2+2] cycloaddition of an alkene double bond to a transition metal alkylidene to form a metallacyclobutane intermediate. The metallacyclobutane produced can then cycloeliminate to give either the original species or a new alkene and alkylidene. Interaction with the d-orbitals on the metal catalyst lowers the activation energy enough that the reaction can, in some special cases, proceed rapidly at modest temperatures (Figure 18). [92]

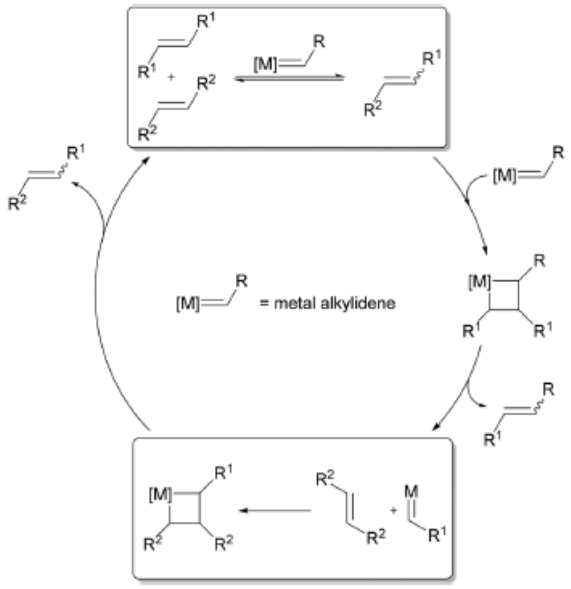

Figure 18: General catalytic cycle of olefin metathesis. [92]

5.1.1 *Types of olefin metathesis*

Olefin metathesis can be classified into six categories: ring closing metathesis (RCM) the opposite reaction of ring opening metathesis (ROM) in which a diene is transformed into a ring; ring-opening metathesis polymerization (ROMP) which involves the opening of cyclic olefins,

generally strained although not always, to give polymeric compounds; cross metathesis (CM), its opposite reaction called ethenolysis and acyclic diene metathesis polymerization (ADMET) used to polymerize terminal dienes to polyenes (Table 4). Asymmetric variants of RCM and ROCM have also been developed. [93]

Table 4: Types of olefin metathesis. [90,93]

Type of olefin matathesis	Scheme of matathesis
RCM	
ROM	
ROMP	
CM	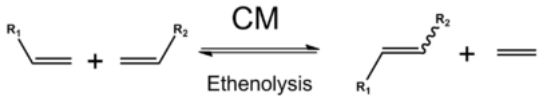
Ethenolysis	
ADMET	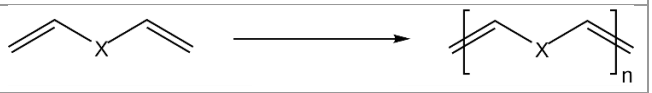

5.1.2 *Catalysts of CM olefin metathesis*

Catalyst systems for the olefin metathesis generally contain a transition metal compound, but often require the presence of a second compound (co-catalyst) and sometimes a third (promoter). [90] Catalyst system commonly used is based on chlorides, oxides, or other easily accessible compounds of molybdenum, ruthenium, wolfram, osmium, iridium and other compounds. Molybdenum soon appeared to be the most suitable metals used for catalysts. Subsequently, some catalysts were produced with this metal, but there was still uncertainty as to what groups would bind to the metal to give stable yet active alkylidene complexes. [90,94]

Since the beginning, intense research in catalyst design for olefin metathesis has been undertaken to address the following issues: **a) Catalyst stability:** In general, a catalyst which is stable in air and moisture and for which there is no need to take any special measurement is always a better choice; **b) Catalyst activity/efficiency:** These are generally characterized by effective turnover number and the effective turnover frequency; **c) Substrate scope and selectivity:** Tolerance for most functional groups, including coordinating atoms such as alcohols, acids, amides, esters, ketones, etc. and also in terms of E/Z selectivity of the generated olefin is always taken into consideration during the reaction. [90,92] Lastly in general, the

higher substituted olefins are less reactive, which implies that the steric bulkiness hampers the incorporation of metal alkylidene into the substrate. [90]

A breakthrough came in 1990 when Schrock et al. [95,96] reported construction of a group very active, well-defined Mo catalysts. Two years later, another breakthrough in the development of metathesis catalysts came when Grubbs et al. [97,98] discovered a catalyst with metallic ruthenium. It was stable in air and demonstrated higher selectivity than Mo catalysts. These new catalyst also had ability to initiate metathesis in the presence of alcohols, water and carboxyl acids. Grubbs catalysts have become the first well-defined catalysts for general metathesis applications in laboratories. [90]

Ruthenium complexes with significantly improved properties were discovered during the early 2000s. Unsaturated N-heterocyclic carbene (NHC) complexes reported by Herrmann, Nolan, and Grubbs exhibited significantly greater metathesis activity and enhanced thermal stability. The saturated NHC complex Ru-2-I, disclosed by Grubbs and coworkers and Hoveyda's phosphine-free variant Ru-2-II, have found widespread use in synthetic organic and polymer chemistry. Notably, Ru-2-I provided the first examples of selective cross-metathesis (CM) reactions. The NHC family of well-defined catalysts has also enabled several metathesis processes on an industrial scale. For example, Simeprevir, a hepatitis C treatment identified as an essential medicine by the World Health Organization, is prepared by RCM. [90,92,94]

For our reaction, at first, the influence of the catalysts on the yield of products was studied by A. Ville, PhD. at SONAS. After this study, 3 ruthenium catalysts were selected: the classical Grubbs catalyst system (Ru-2) and another catalyst system with a similar structure named Hoveyda-Grubbs (Hg-1 and Hg-2). These catalysts developed by Hoveyda et al. are stable ruthenacarbenes derived from Grubbs complexes. [99] In these catalysts, benzylidene and tricyclohexylphosphine have been replaced by a bidentate benzylidene ether ligand which exhibits excellent thermal stability as well as greater tolerance to oxygen and moisture.

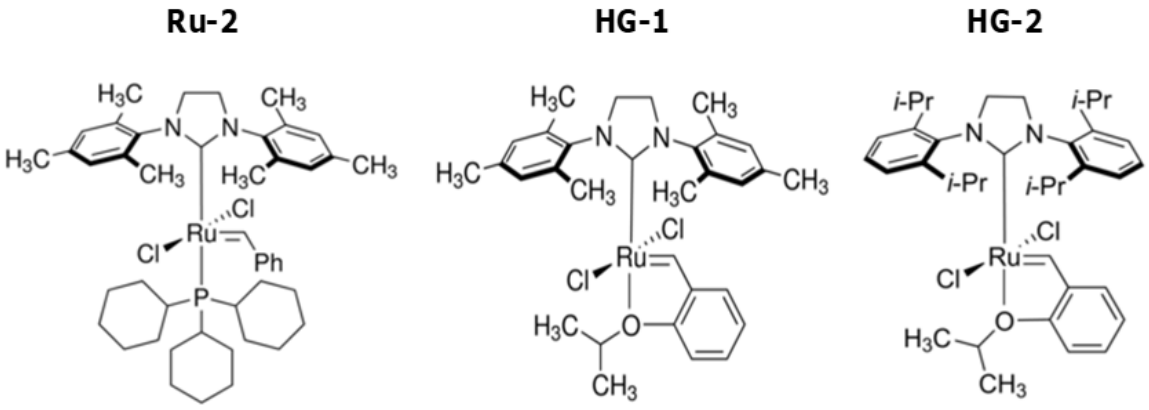

Figure 19: Structure of catalysts used in metathesis reaction. [100-102]

5.2 HPLC analysis

HPLC analysis is not so common method in organic synthesis. In my case, this method of HPLC analysis of reaction mixtures was basically used to estimate experimental products' yields without purification and only a small amount of the reaction mixture (60 µL) was used for the analysis. Consequently, the yields of the products were computed from area of peaks in chromatograms with simple equations listed below. The peaks were compared with peaks of standards and the percentage purity of standards was also included in the calculations.

The RP-HPLC mobile phase consisted in water + 0.1% formic acid (solvent A) and methanol + 0.1% formic acid (solvent B). The solvent gradient was as follows (starting with 15 % solvent A): 0 min, 85 % B; 7 min, 90 % B; 12 min, 95 % B; 21 min, 100 % B; 27 min, 85 % B. The flow rate was 1 mL/min, the injection volume was 20 µL (standards only 10 µL) and was made in triplicates, and the eluent detection was achieved at 254 and 296 nm. All HPLC analyses were performed at 25 °C.

Preparations of HPLC samples: HPLC analysis was underway always right after 1, 3, 5 and 7 days of reaction. Firstly, the amount of evaporated solvent ($CDCl_3$) had to be added to reaction mixture (RM) (usually less than 0.05 mL). Afterwards, 60 µL of RM was transferred to snap-cap microtube where the solvent was carefully evaporated with stream of nitrogen. 500 µL of HPLC grade methanol was added and the solution was centrifugated for 10 minutes at 3500 rpm. The supernatant was transferred to a HPLC vial and analyzed.

The series of equations applied in calculation of percentage of products yields were as follows:

$$mass\ in\ injection\ [\mu g] = \frac{peak\ area\ [in\ millions] \cdot mass\ of\ S}{peak\ area\ of\ S}$$

$$mass\ in\ RM\ sample\ [\mu g] = \frac{mass\ in\ injection \cdot volume\ of\ RM\ sample\ (500\ \mu L)}{volume\ of\ injection\ (20\ \mu L)}$$

$$mass\ in\ RM\ [\mu g] = \frac{mass\ in\ RM\ sample \cdot volume\ of\ total\ RM\ (700\ \mu L)}{volume\ of\ RM\ (60\ \mu L)^{3}} \cdot 1000$$

$$yield\ [\%] = \frac{mass\ in\ RM}{MW\ \cdot n\ of\ TsOT3} \cdot 100$$

S	standard
RM	reaction mixture
MW	molecular weight
n	amount of substance in mmol

5.3 Reaction under microwave irradiation

Several experiments with all three types of catalysts were also performed in a microwave reactor after the main reaction was optimized. The reason was an even greater acceleration of the reaction time.

Microwave-assisted heating under controlled conditions has been shown to be a valuable technology for medicinal chemistry and drug discovery applications. Microwave reactors allow fast heating of reaction mixtures to high pressures and temperatures – far above the boiling point of the used solvents. [103] Employing closed vessel conditions dramatically reduces reaction times typically from days or hours to minutes or even seconds. [103-105] This rate acceleration is based on the Arrhenius law, which states as a rule of thumb that the reaction rate is doubled when increasing the reaction temperature by 10 °C. [104]

Microwave chemistry is based on the efficient heating of materials (in most cases solvents) by dielectric heating effects. Dielectric heating works by two major mechanisms (Figure 20):

[3] volume of RM used for preparation of RM HPLC sample

- Dipolar polarization

For a substance to be able to generate heat when irradiated with microwaves it must be a dipole, i.e. its molecular structure must be partly negatively and partly positively charged. Since the microwave field is oscillating, the dipoles in the field align to the oscillating field. This alignment causes rotation, which results in friction and ultimately in heat energy. [103-105]

- Ionic conduction

During ionic conduction, dissolved charged particles (usually ions) oscillate back and forth under the influence of microwave irradiation. This oscillation causes collisions of the charged particles with neighbouring molecules or atoms, which are ultimately responsible for creating heat energy. [103-106]

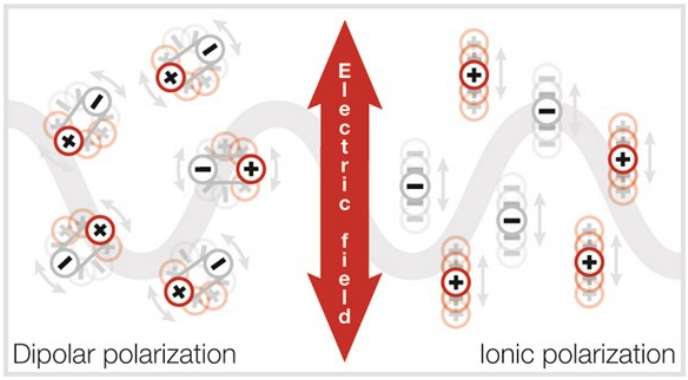

Figure 20: Illustration of the two main dielectric heating mechanisms: dipolar polarization and ionic conduction. [104]

The conversion of electromagnetic energy into heat energy works highly efficiently and results in extremely fast heating rates which are not reproducible with conventional heating. [104,105] Due to the rapid heating to the target temperature, the formation of by-products is suppressed. This is another huge advantage of microwave heating, since it means that higher product yields can be achieved and the purification is simplified. [105,106]

6 Deprotection of p2-p4 products

Usage of only one step deprotection with potassium hydroxide (2M aqueous solution) in tetrahydrofuran (THF)/MeOH (2:1) was the first idea. After a few unsuccessful attempts with products' degradation after several hours of reaction we decided to carry out a two-step deprotection with lithium hydroxide in the first step of basic hydrolysis of methyl ester and potassium hydroxide (2M aqueous sol.) in a second step for deprotection of tosyl group.

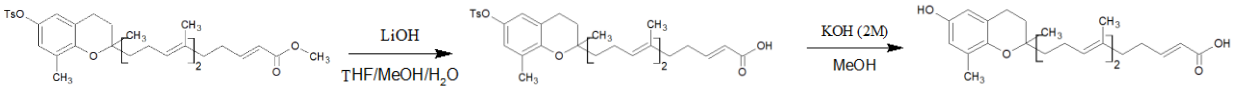

Figure 21: Scheme of two-step deprotection. [89]

1st step:

Purified product (p2, p3 and p4) was dissolved in mixture of THF/MeOH/H_2O (3:1:1) and lithium hydroxide (4.33 eq.) was added. The reaction was stirred at 40°C. The time of reaction depended on the length of the side chain – p2 20 hours, p3 17 hours and p4 6 hours. The completion of reaction was checked by TLC (UV light and CAM stain) with PE/Ac/DCM (7:2:1) as a mobile phase. The reaction was quenched with 10% hydrochloric acid, extracted three times with ethyl acetate. The pooled organic layers were twice washed with water and once with brine, dried over anhydrous sodium sulfate and filtered. The solvent was removed under reduced pressure. Yields were as follows: 90 % of p2; 90 % of p3, 91 % of p4.

2nd step:

Product from 1st deprotection step was dissolved in MeOH and potassium hydroxide (2M aqueous solution) (20 eq.) was added. The reaction was stirred 6 hours at 70°C and 12 hours overnight without heating. The completion of reaction was checked by TLC (UV light and CAM stain) with PE/Ac/DCM (7:2:1) as a mobile phase. The reaction was quenched with 10% hydrochloric acid, extracted three times with diethyl ether. The pooled organic layers were twice washed with water and once with brine, dried over anhydrous sodium sulfate and filtered. The solvent was removed under reduced pressure. p2 and p3 were purified by preparative TLC on silica gel, and p4 was purified by normal phase column chromatography. Yields of completely deprotected products were as follows: 31 % of p2; 16 % of p3, 17 % of p4.

7 Additional reactions

Verification and application of the most efficient metathesis reaction with MA on different starting T3 derivatives was another aim of my work. In these cases, we did not need exact numbers of yields.It was always important to consume the majority of starting compounds during reactions. During these examinations, the advantage of HPLC analysis was not taken, only TLC chromatography was used to evaluate completion of the reaction.

Due to the speed of the reactions, the optimal conditions in microwave reactor were utilized, i. e. 1 hour at 100°C for the examination. 2.4 equivalents of the reactants were used during the experiments.

7.1 4-pentenoic acid

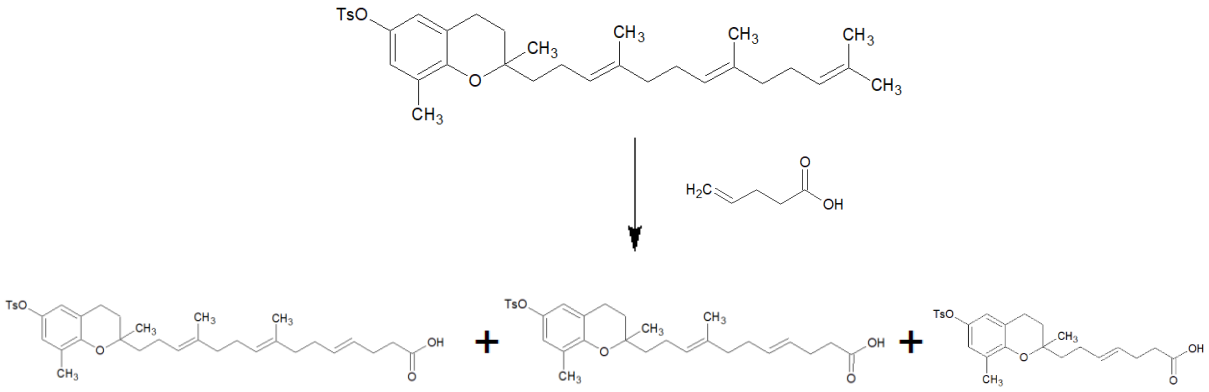

Figure 22: Scheme of the reaction with 4-pentenoic acid. [89]

First reaction was the reaction of already prepared TsOδT3 with 4-pentenoic acid (97%, Sigma-Aldrich). To a solution of TsOδT3 (30 mg; 0.05 mmol; 1 eq.) in 0.7 mL of $CDCl_3$ were added 4-pentenoic acid (12.25 µL; 0.12 mmol; 2.4 eq.) and Grubbs catalyst Hg-1 (3.13 mg; 0.005 mmol; 0.1 eq.). The reaction mixture was stirred under microwave irradiation for 2 h at 100°C and 45 min at 120°C with addition of 0.1 eq. of catalyst. Every hour, TLC chromatography with cyclohexane/ethyl acetate (7:2) as a mobile phase was carried out (UV light and CAM staining was used for observing the spots). After 2 hours and 45 min the reaction was quenched because no starting material was detected on TLC. Work-up and purification on preparative TLC were achieved the same way as the main reaction. Six fractions (1.8 mg – 9.3 mg) were obtained and all of them were analyzed by ^{1}H NMR. Unfortunately, no trace of the expected product was obtained.

There was an idea that the dysfunctionality of the reaction could be caused by an acid that could possibly destroy the sensitive catalyst which is an essential part for CM olefin reaction. Therefore, the esterification of 4-pentenoic acid was carried out.

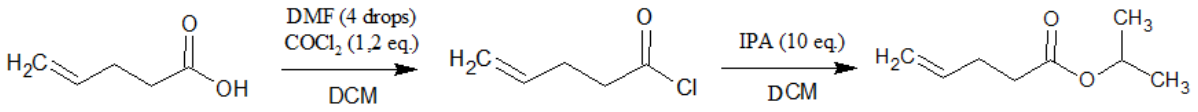

Figure 23: Scheme of esterification of 4-pentenoic acid. [89]

In a dry flask, 4-pentenoic acid (509.7 µL; 4.99 mmol; 1 eq.) was dissolve in 25 mL of dry DCM under ice cooling and nitrogen atmosphere. Oxalyl chloride (5.11 µL; 5.99 mmol; 1.2 eq.) and 4 drops of dimethylformamide were added. The reaction was stirred 3 hours at room temperature under nitrogen atmosphere. Consequently, isopropanol (3.815 mL; 49.9 mmol; 10 eq.) was added and the reaction mixture was stirred 1 hour 15 min at room temperature. Every hour, TLC chromatography with cyclohexane/ethyl acetate (7:2) as a mobile phase was carried out (UV light and potassium permanganate stain was used to visualize the spots). When the reaction was terminated, the reaction mixture was washed three times with saturated aqueous solution of sodium bicarbonate and pooled organic layers were dried over anhydrous sodium sulphate, filtered and evaporated under reduced pressure. The residue was twice distilled and isopropyl ester of 4-pentenoic acid was obtained in 25% yield. The purity of the compound was verified by ^{1}H NMR.

Isopropyl ester of 4-pentenoic acid was utilized in a reaction with TsOδT3 instead of 4-pentenoic acid. The same preparation and the same conditions of reaction were followed. Every hour, TLC chromatography with PE/Ac/DCM (9:1:0.5) as a mobile phase was carried out (UV light and CAM staining was used to visualize the spots). After 3 hours, 0.1 eq. of catalyst was added. And after another hour, the reaction was quenched because no starting material was detected on TLC. Work-up and purification on preparative TLC were prepared the same way as the main reaction. Seven fractions (1.6 mg – 7.3 mg) were obtained and all of them were analyzed by ^{1}H NMR. Unfortunately, no trace of the expected product was obtained.

7.2 Tosylated methyl ester of δ-garcinoic acid + methacrylate

Firstly, tosylated methyl ester of δ-garcinoic acid (δTsO-GA-ME) was synthesized. Again, it was necessary to protect sensitive phenol function in position C6 on chromanol ring. δ-GA-ME had been already prepared from the previous work of Alexia Ville, PhD.; thus, I could use it as

a starting material for tosylation. The same conditions of reaction were followed as for protecting δT3 (Chapter IV.2). The purification of reaction mixture was necessary and it was carried out by column chromatography with mixture of eluents PE/ethyl acetate (8:2). Solvent of pooled tubes after purification was evaporated under reduced pressure and pure δTsO-GA-ME was obtained in 75% yield. Its purity was verified by ^{1}H NMR.

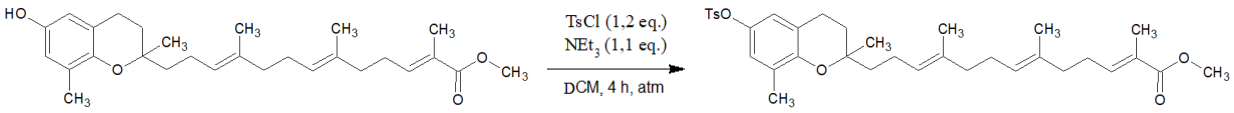

Figure 24: Scheme of protection of δ-GA-ME. [89]

Subsequently, the similar conditions as for the main reaction were applied for reaction of δTsO-GA-ME methacrylate. To a solution of δTsO-GA-ME (30 mg, 0.05 mmol, 1 equiv.) in degassed deuterated chloroform (0,7 mL) were added methacrylate (10.8 µL, 0.12 mmol, 2.4 equiv.) and Ru-2 catalyst (4.2 mg, 0.005 mmol, 0.1 equiv.). The reaction mixture was stirred in microwave reactor for 1 hour at 100°C. TLC was carried out with cyclohexane/ethyl acetate (7:2). Then the work-up was performed the similar way as metathesis reaction (p. 41). Then the solvent was removed under reduced pressure. The residue was purified by preparative TLC on silica gel eluted with a cyclohexane/ethyl acetate mixture 7:2 to afford six fractions which were analyzed by ^{1}H NMR. Fraction n.4 corresponded with **p3** product (yield 21 %) and fraction n. 5 with **p4** product (yield 48 %). Nevertheless, the purity of the purified compounds required further optimization. An option could be the use of reverse phase. The synthesis of these new garcioc acid analogues was already a preliminary success.

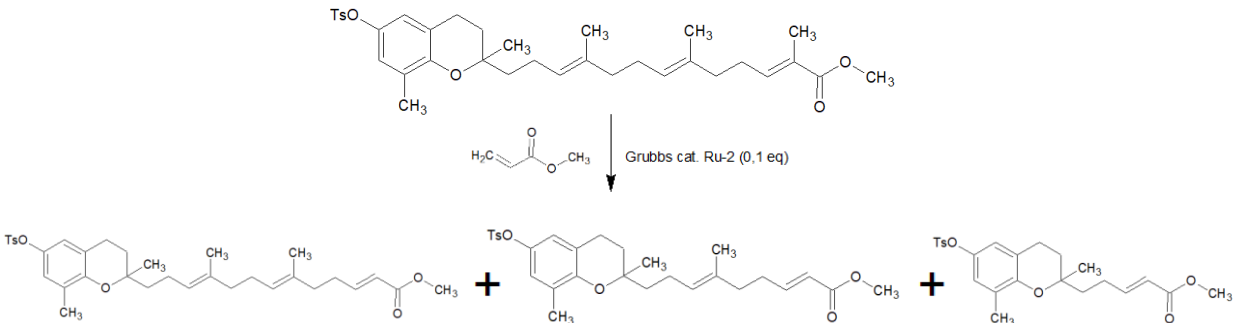

Figure 25: Scheme of reaction of δTsO-GA-ME with methacrylate. [89]

7.3 2-methylenepropane-1,3-diyl diacetate

Firstly, the reactant had to be synthesized. To a solution of the commercial 2-methylene-1,3-propanediol (278 µL, 3.4 mmol, 1 equiv.) in dichloromethane (10 mL) were added acetic anhydride (1.3 mL, 13.6 mmol, 4 equiv.), pyridine (1.4 mL, 17 mmol, 5 equiv) and 4-(dimethylamino)pyridine (42 mg, 0.34 mmol, 0.1 equiv). The reaction mixture was stirred at room temperature for 24 h. Then the reaction was quenched with 10% aqueous solution of hydrochloric acid. The resulting mixture was extracted three times with diethyl ether. The combined organic layers were washed with water and brine, dried over anhydrous sodium sulfate, filtered and concentrated under reduced pressure. The crude product was obtained as a yellow liquid and can be used in the next step without further purification. Yield 98 %.

Figure 26: Scheme of synthesis of 2-methylenepropane-1,3-diyl diacetate. [89]

α-tocotrienol had to be synthesized from δ-tocotrienol, because we obtained enough δT3 by the purification of *Bixa orellana* extract. Alkylation in positions on C5 and C7 on a chromanol ring was achieved by di-Mannich reaction. This is an example of nucleophilic addition which consists of an amino alkylation.

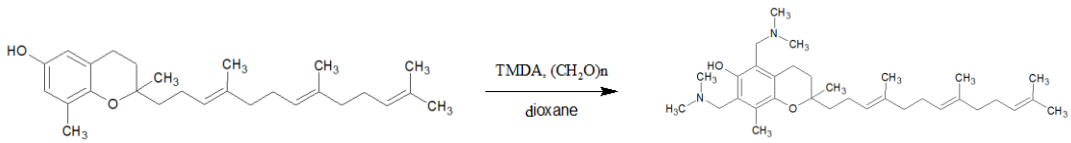

Figure 27: Scheme of di-Mannich reaction. [89]

To a solution of δT3 (1 g; 2.52 mmol; 1 eq.) in 1,4-dioxane (30 mL) were added tetramethyldiaminomethane (TMDA) (6.9 mL; 50.43 mmol; 20 eq.) and paraformaldehyde (1.5 g; 50.43 mmol; 20 eq.) The reaction was stirred 19 hours at 100°C. TLC was carried out DCM/MeOH (9:1) as a mobile phase (UV light and CAM staining were used to visualize the spots). The RM was evaporated under reduced pressure. Yield of product was 98 %.

Then, the two-step reduction of two 2-(dimethylamino)ethyl groups in position C5 and C7 on a chromanol ring was carried out. First reduction was not successful because only one group was reduced; therefore, the reaction had to be repeated in similar conditions.

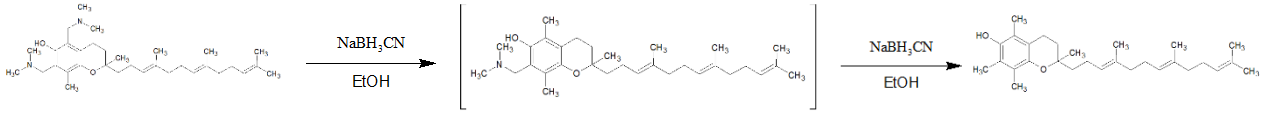

Figure 28: Scheme of reduction. [89]

The product from previous reaction (1.3 mg; 2.46 mmol; 1 eq.) was dissolved in 38 mL of ethanol and sodium cyanoborohydride (4.6 g; 73.74 mmol; 30 eq.) was added. The reaction was stirred 8 hours under nitrogen atmosphere. TLC was carried out with PE/ethyl acetate (9:1) as a mobile phase and UV light and CAM stains were used to visualize the spots on TLC. The reaction was quenched with water and diethyl ether and extracted three times with diethyl ether. Pooled organic layers were washed twice with water and once with brine and then dried over with anhydrous sodium sulfate and filtered. The solvent was removed under reduced pressure. The product had to be purified by column chromatography with eluents PE/ethyl acetate (9:1).The purity and identification of four obtained fractions were realized by ^{1}H NMR. αT3 was obtained in 40% yield, and also βT3 in 9% yield was gained as a by-product of the reaction. The remaining fractions were pooled together because both of them contained partially reduced product and therefore, the reduction had to be repeated. Thanks to second reduction, another 10% yield of αT3 was obtained.

Again, the sensitive hydroxyl group on C6 on the chromanol ring had to be protected. Therefore the tosylation was used for its protection. The same conditions of reaction were followed as tosylation in chapter IV.2.

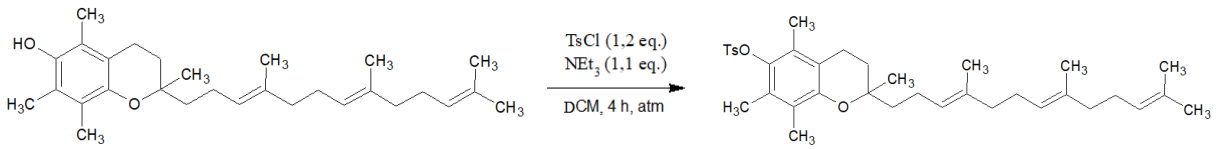

Figure 29: Scheme of tosylation of αT3. [89]

A problem occurred during difficult purification by column chromatography with eluents cyclohexane/ethyl acetate (9:1) when the separation of tosylated αT3 and reactant 4-toluensulfonylchloride failed. ^{1}H NMR revealed approximately 30% contamination of 4-toluensulfonyl chloride. Despite this, the contaminated product was used for further reaction.

Next metathesis reaction was attempted with different reactant - methylenepropane-1,3-diyl diacetate was used instead of MA. The same 2.4 equivalence of reactant was preserved and

Grubbs catalyst Ru-2 was chosen. The reaction was conducted 1 hour under microwave irradiation at 100°C, 1 hour at 150°C and another 1 hour at 150°C with addition of 0.1 eq. catalyst and 1.2 eq. of methylenepropane-1,3-diyl diacetate. TLC was carried out every 1 hour but it did not change at al. ^{1}H NMR proved a consumption of TsCl (a contamination), but majority of TsOαT3 still remained in reaction mixture. After this failure, the reaction was terminated. Any of desired products was synthesized, it was probably due to the large contamination of 4-toluensulfonyl chloride, which apparently disrupted the reaction.

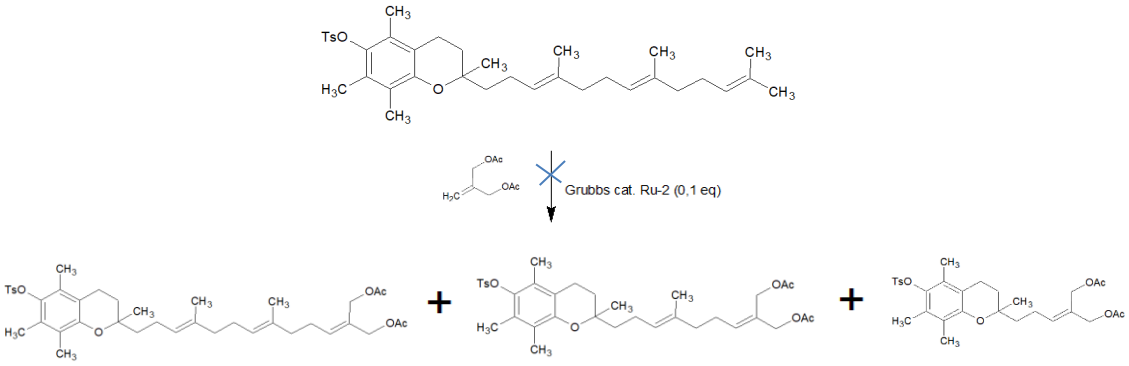

Figure 30: Scheme of reaction of TsOαT3 with 2-methylene-1,3-propanediol. [89]

V. Results of optimization

My results follow the work of Alexia Ville, PhD. who started optimizing conditions one year ago. Her first result was achieved with Ru-2 Grubbs catalyst, 1.2 eq. of MA and the reaction was conducted at 70°C and lasted 7 days. Improvement of these conditions and reduction of time were my main goal.

1 Results according to the type of catalyst

At first, I decided to compare the estimated yields calculated from peak areas from HPLC analysis of products p2 – p4 according to used catalyst during reaction. HPLC analysis was carried out after 3, 5 and 7 days of reaction. The reaction with 2.4 eq. of MA was terminated after 3 days due to decreasing product yields with additional days of running reaction and also because we needed some higher amount of products for next steps of the work.

1.1 Yields of products with Grubbs catalyst Ru-2

Table 5: Comparison of estimated yields – Ru-2 catalyst.

Estimated yield calculated by HPLC analysis in %				
MA eq.		**3 days**	**5 days**	**7 days**
0.6	**p2**	5.6	5.1	4.1
	p3	10.5	9.5	7.9
	p4	11.9	10.6	9.1
0.8	**p2**	14.3	13.6	11.6
	p3	12.5	11.4	10.0
	p4	10.3	9.0	8.1
1.2	**p2**	19.7	17.1	14.1
	p3	21.6	18.7	15.3
	p4	19.4	15.9	13.1
2.4	**p2**	9.7	N/A	N/A
	p3	26.2	N/A	N/A
	p4	39.0	N/A	N/A

Ru-2

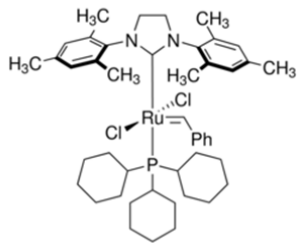

1.2 Yields of products with Grubbs catalyst Hg-1

Table 6: Comparison of estimated yields – Hg-1 catalyst.

Estimated yield calculated by HPLC analysis in %				
MA eq.		**3 days**	**5 days**	**7 days**
0.6	**p2**	2.2	1.9	1.6
	p3	4.7	4.1	3.2
	p4	5.9	5.3	4.4
0.8	**p2**	8.9	8.2	10.2
	p3	9.9	9.7	12.7
	p4	7.6	7.7	10.2
1.2	**p2**	5.5	4.9	3.9
	p3	11.3	10.4	8.3
	p4	11.9	11.2	9.1
2.4	**p2**	15.3	N/A	N/A
	p3	29.6	N/A	N/A
	p4	32.8	N/A	N/A

HG-1

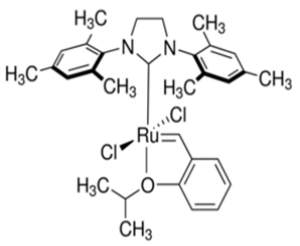

1.3 Yields of products with Grubbs catalyst Hg-2

Table 7: Comparison of estimated yields – Hg-2 catalyst.

Estimated yield calculated by HPLC analysis in %				
MA eq.		**3 days**	**5 days**	**7 days**
0.6	**p2**	11.2	7.2	5.3
	p3	13.9	7.4	6.1
	p4	11.6	6.1	5.1
0.8	**p2**	14.9	6.7	8.2
	p3	20.0	6.1	8.5
	p4	16.9	5.1	7.1
1.2	**p2**	10.0	3.1	3.5
	p3	24.0	5.1	5.9
	p4	23.8	4.8	6.1
2.4	**p2**	18.1	N/A	N/A
	p3	31.2	N/A	N/A
	p4	43.1	N/A	N/A

HG-2

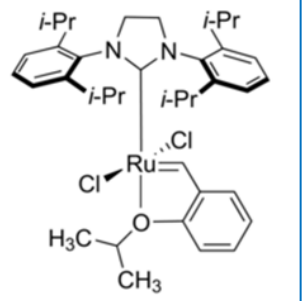

It is evident from the tables of estimated yields that the highest yields were obtained after 3 days of reaction using 2.4 eq. of MA (Chart 1). It can also be seen from the tables that yields decrease over time; thus, the reaction with 2.4 eq of MA was terminated right after 3 days. Accordingly, I prepared the chart which compared products' yields with type of catalyst. Thanks to these results, we decided to decrease the time to 1 day and carry out the reaction again with all three types of catalysts. (Chapter V.1.1.4)

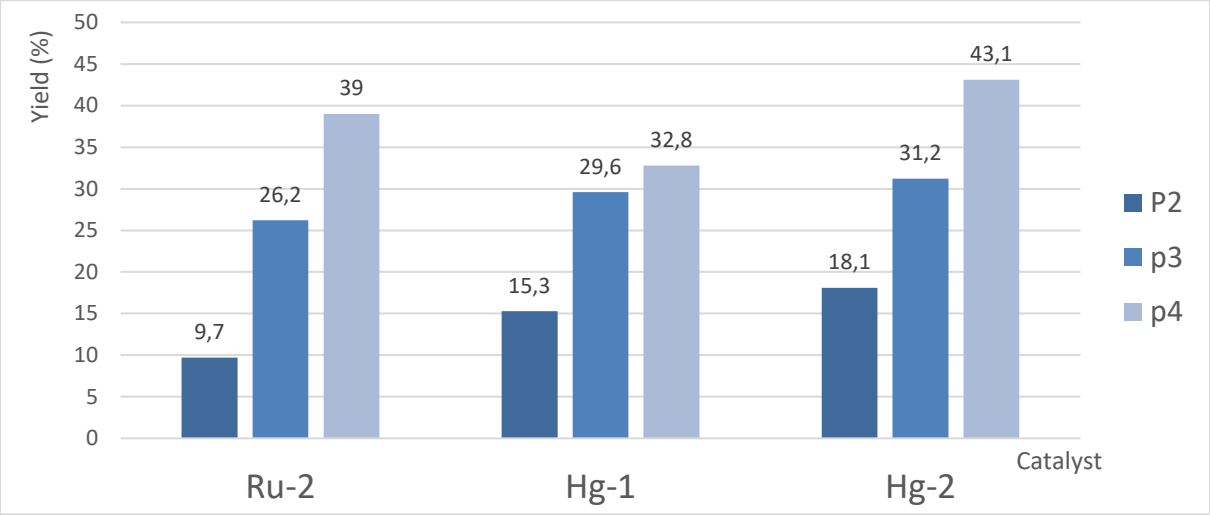

Chart 1: Comparison of the highest yields – 2.4 eq. of MA, 3 days.

Results after 3 days and 1.2 eq. of MA are also interesting. Yields of products from reaction with Ru-2 catalyst are very balanced (around 20% yield), unlike to reaction with 2.4 eq. of MA. Although, these yields are not very high, achievement of product balanced yields was also the intention of our effort. (Chart 2)

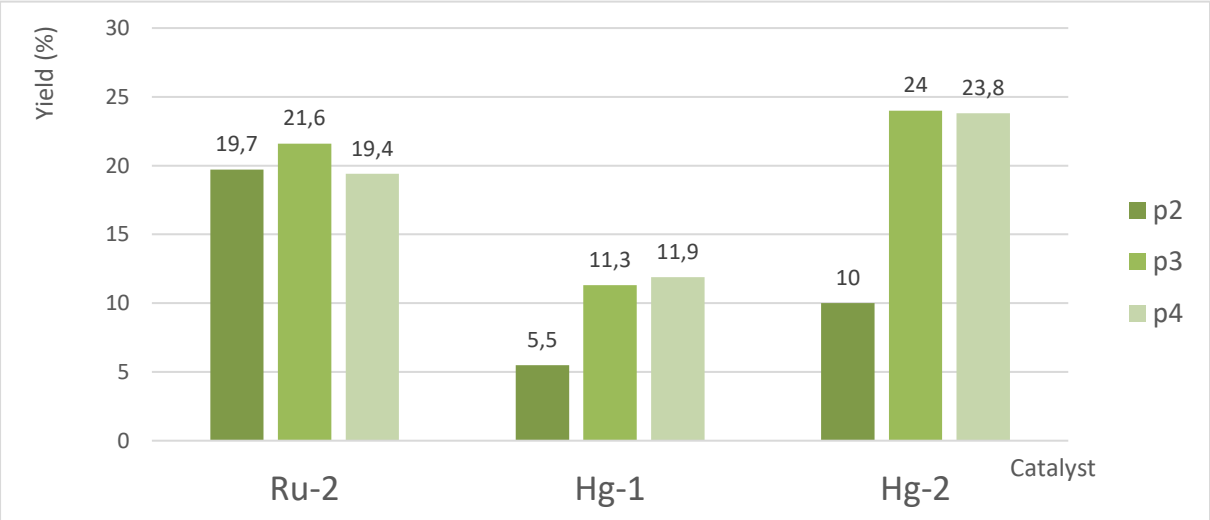

Chart 2: Comparison of the yields – 1.2 eq. of MA, 3 days.

2 Yields of products after 1day reaction

Table 8: Comparison of estimated and real yield after 1 day, 2.4 eq. of MA.

Estimated yield calculated by HPLC analysis in %				
MA eq.		**Ru-2**	**Hg-1**	**Hg-2**
2.4	**p2**	10.5	26.4	6.2
	p3	23.2	28.9	18.4
	p4	39.0	39.4	37.9
Real yield obtained by preparative TLC in %				
2.4	**p2**	12	16	9
	p3	25	27	24
	p4	51	39	45

Chart 3: Comparison of estimated and isolated yields after 1day reaction with 2.4 eq. of MA.

The reaction after 1 day showed interesting data. Estimated yields mostly corresponded to estimated yields after 3 days (it is possible to find exceptions, e.g. yield of p2 Hg-1 cat. = 15 % after 3 days, 26 % after 1 day; yield of p2 Hg-2 cat. = 18 % after 3 days, 6 % after 1 day). But in these case, the yields obtained after preparative TLC purification varied from estimated yields, the isolated yields were actually higher (just with one exception, the real yield of p2 Hg-1 is 10% lower).

3 Reaction in a microwave reactor

The reactions with the best yields (2.4 eq. of MA) were repeated under microwave irradiation and they were realized with all three types of catalysts. The reactions were conducted for 1 hour at 100°C.

Table 9: Estimated yields – reaction in a microwave reaction.

Estimated yield calculated by HPLC analysis in %				
MA eq.		**Ru-2**	**Hg-1**	**Hg-2**
2.4	**p2**	19	8	nd[4]
	p3	22	3	nd
	p4	24	11	nd

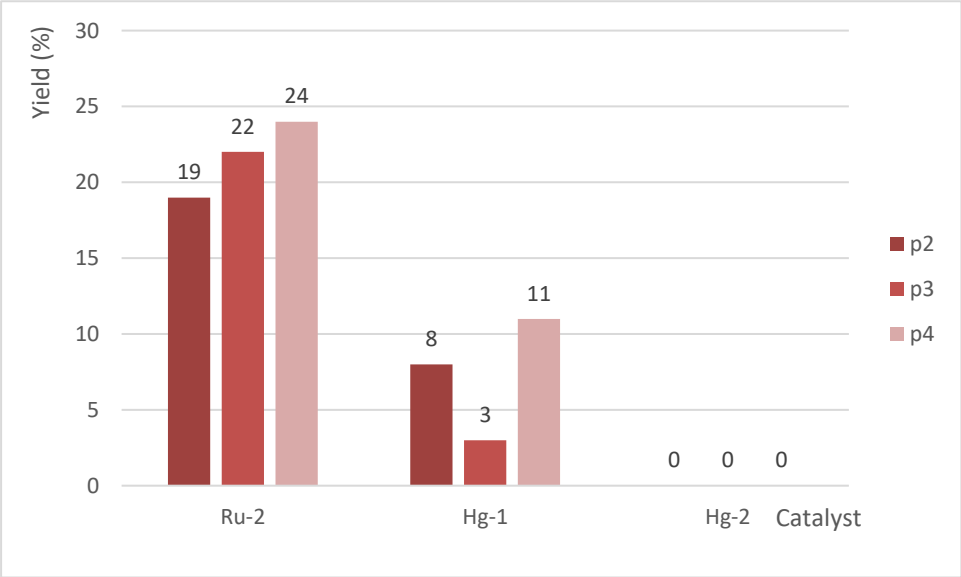

Chart 4: Comparison of estimated yields – reaction in a microwave reactor.

[4] Not detected

From the table (9) and the chart (4), it is obvious that the most effective catalyst was definitely Ru-2 catalyst. With Ru-2, the products were synthesized in very balanced ratio. It is quite unusual that Hg-2 catalyst did not work at all; HPLC analysis did not prove any formations of products.

Table 17 that summarizes all the reactions and their conditions performed during optimization can be found in the appendix.

VI. Discussion and Conclusion

During my work, I synthesized 3 new compounds – new analogues of vitamin E which were sent to Jena to evaluate their inhibitory activity *in vitro* on purified 5-LOX and polymorphonuclear leucocytes.

Their conditions of semisynthesis were optimized using HPLC analysis to evaluate the consumption of the starting material. Because 3 products were formed during the reaction, the results can be viewed from multiple points of view. A) The highest yields of particular product could be compared, B) the highest yields of all products during one reaction could be determined or C) we could find the effective conditions where the balanced ratio of products was formed.

A) The highest yields of particular product:

   p2: The highest yield of p2 (20 %) product was obtained after **3-day** reaction, carried out at 70°C with **Ru-2** Grubbs catalyst and **1.2 eq.** of methacrylate were used. (Table 5)

   p3: The highest yield of p3 (31 %) product was obtained after **3-day** reaction, carried out at 70°C with **Hg-2** catalyst and **2.4 eq.** of methacrylate were used. (Table 7)

   p4: The highest yield of p4 (51 %) product was obtained after **1-day** reaction, carried out at 70°C with **Ru-2** catalyst and **2.4 eq.** of methacrylate were used. (Table 8)

B) The highest yields of all products (p2 = 18 %, p3 = 31 % , p4 = 43 %) in one reaction were obtained after **3-day** reaction, carried out at 70°C and **Hg-2** catalyst and **2.4 eq.** of methacrylate. (Table 7) (Appendix – MS14 3 days)

C) Balanced ratio of products:

   - Firstly, the balanced yields of products (p2 = 19 %, p3 = 22 % and p4 = 24 %) were obtained after **1-hour** reaction, carried out under **microwave irradiation** at 100°C with **Ru-2** catalyst and **2.4 eq.** of methacrylate. (Table 9) (Appendix – MS45 1 hour)

- Secondly, the balanced yields of products (p2 = 20 %, p3 = 22 % and p4 = 19 %) were obtained after **3-day** reaction, carried out at 70°C with **Ru-2** catalyst and **1.2 eq.** of methacrylate. (Table 5) (Appendix – MS19 3 days)

The collected and purified products (p2-p4) were effectively deprotected thanks to 2-step deprotection and final compounds could be sent for testing.

For the additional reactions where we would like to verify that the optimized conditions could be efficient with other reactants, the reaction conditions identified under microwave irradiation were utilized because of balanced ratio of products and also because of shorter reaction time. Unfortunately, these conditions of semisynthesis were not applicable for the reaction derivatives of T3 and δ-garcinoic acid.

The reaction TsOδT3 with 4-pentenoic acid was unsuccessful probably due to acidity of reactant which disturbed the function of Grubbs catalyst and we were not able to synthesize any of our desired products. Esterification of acid to isopropyl ester of 4-pentenoic acid also did not prevent the failure of reaction.

The second reaction when tosylated methyl ester of δ-garcinoic acid reacted with methacrylate was partly efficient – it was possible to synthesize two of three products, exactly one double bond side chain p4 and the two double bonds side chain p3 products which was obtained in 48% and 21% yield, respectively. If we had wanted to work with these products further, another purification would have been needed.

The third reaction, which was quite complicated for preparation of starting material TsOαT3 from δT3, unfortunately also failed. The last step before the last reaction in this series, where TsOαT3 reacted with 2-methylenepropane-1,3-diyl diacetate, was ruined by very inefficient purification of TsOαT3. After the purification, TsOαT3 was still contaminated with approximately 30 % of 4-toluensulfonyl chloride. Because of time constraints I was unable to repeat the purification and, therefore, the contaminated product had to be used for the last reaction. No desired products were obtained, mainly and apparently due to the high contaminated of starting material. This reaction would certainly be worth repeating during next studies.

VII. Organic synthesis

TsOδT3

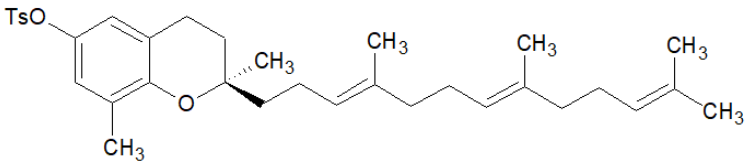

(2*R*)-2,8,-dimethyl-2-[(3*E*,7*E*)-4,8,12-trimethyldeca-3,7,11-trien-1-yl]-3,4-dihydro-2H-1-benzopyran-6-yl 4-methylbenzene-1-sulfonate

Molecular weight = 550.3117 g/mol

To a solution of δ-tocotrienol (600 mg; 1.51 mmol; 1 eq.) in dichloromethane (33 mL) were added 4-toluenesulfonyl chloride (316.5 mg; 1.66 mmol; 1.1 eq.) and trimethylamine (252.2 µl; 1.81 mmol; 1.2 eq.). The reaction mixture was stirred at room temperature for 4 hours. Then the reaction was quenched with saturated aqueous solution of sodium bicarbonate, after extracted 3 times with diethyl ether. The combined organic layers were washed twice with water and once with brine and afterwards dried over anhydrous sodium sulfate, filtrated through the cotton and evaporated under reduced pressure. The residue was purified by automated flash chromatography on silica gel eluted with mixture of petroleum ether/acetone (9:1). The desired product was obtained in 60% yield.

Light brown oil, R_f = 0.43 (petroleum ether/acetone 8:2)

^{1}H NMR (400 MHz, $CDCl_3$) δ 7.72 (d, *J* = 8.4 Hz, 2H), 7.31 (d, *J* = 7.9 Hz, 2H), 6.56 (d, *J* = 2.6 Hz, 1H), 6.52 (d, *J* = 2.4 Hz, 1H), 5.14-5.07 (m, 3H), 2.67-2.63 (m, 2H), 2.45 (s, 3H), 2.13-2.02 (m, 6H), 2.05 (s, 3H), 1.99-1.94 (m, 4H), 1.82-1.70 (m, 2H), 1.67 (s, 3H), 1.64-1.52 (m, 2H), 1.59 (s, 3H), 1.58 (s, 6H), 1.25 (s, 3H).

^{13}C NMR (100 MHz, $CDCl_3$) δ 150.8, 145.1, 141.5, 135.5, 135.2, 132.9, 131.4, 129.7 (2 C), 128.7 (2 C), 127.6, 124.5, 124.2, 124.1, 122.0, 121.2, 120.3, 76.3, 39.9, 39.8 (2 C), 31.0, 26.9, 26.7, 25.9, 24.2, 22.4, 22.2, 21.8, 17.8, 16.2, 16.1, 16.0.

IR (neat) *vmax* 2919, 2853, 1473, 1449, 1373, 1189, 1093, 984, 813, 581 cm^{-1}.

General procedure for the Grubbs metathesis to δT3 derivatives

To a solution of TsOT3 (30 mg; 0.05 mmol; 1 equiv.) in degassed deuterated chloroform (0.7 mL) were added methylacrylate (10.8 µL; 0.12 mmol; 2.4 equiv.) and Hg-2 catalyst (3.55 mg; 0.005 mmol; 0.1 equiv.). The reaction mixture was stirred for 3 days. Then the solvent was removed under reduced pressure. The residue was purified by preparative TLC on silica gel with a cyclohexane/ethyl acetate mixture 7:2 as a mobile phase to afford the desired products as light oil.

p2

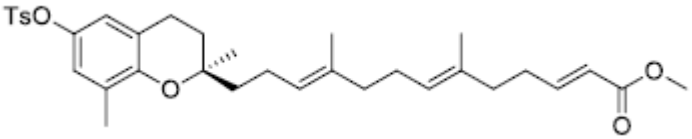

Mw = 580.7746 g/mol

methyl(2*E*,6*E*,10*E*)-13-[(*R*)-2,8-dimethyl-6-[(4-methylbenzenesulfonyl)oxy]-3,4-dihydro-2H-1-benzopyran-2-yl]-6,10,-dimethyltrideca-2,6,10-trienoate

Yellow oil; 10% yield; Rf = 0.58 (cyclohexane/ethyl acetate 7:2).

^{1}H NMR (400 MHz, $CDCl_3$) δ 7.72 (d, *J* = 7.8 Hz, 2H), 7.31 (d, *J* = 8.0 Hz, 2H), 6.98-6.91 (m, 1H), 6.56 (s, 1H), 6.52 (s, 1H), 5.81 (d, *J* = 15.5 Hz, 1H), 5.14-5.10 (m, 2H), 3.72 (s, 3H), 2.69-2.61 (m, 2H), 2.45 (s, 3H), 2.31-2.26 (m, 2H), 2.12-2.08 (m, 6H), 2.05 (s, 3H), 1.98-1.94 (m, 2H), 1.82-1.70 (m, 2H), 1.67-1.50 (m, 2H), 1.58 (s, 6H), 1.25 (s, 3H).

^{13}C NMR (100 MHz, $CDCl_3$) δ 167.3, 150.8, 149.5, 145.1, 141.5, 136.3, 133.6, 133.0, 129.7 (2C), 128.7 (2C), 127.6, 125.3, 124.2, 122.0, 121.2, 121.0, 120.3, 76.3, 51.6, 39.9, 39.7, 38.0, 31.0, 30.9, 26.6, 24.2, 22.4,22.2, 21.9, 16.2, 16.1, 16.0.

IR (neat) *vmax* 2925, 2852, 1722, 1473, 1450, 1371, 1189, 1174, 1093, 984 cm^{-1}.

---

p3

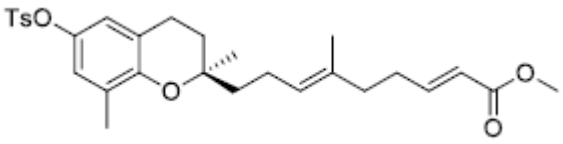

Mw = 512.6575 g/mol

methyl(2*E*,6*E*)-9-[(2*R*)-2,8-dimethyl-6-[(4-methylbenzenesulfonyl)oxy]-3,4-dihydro-2H-1-benzopyran-2-yl]-6-methylnona-2,6-dienoate

Yellow oil; 30% yield; Rf = 0.53 (cyclohexane/ethyl acetate 7:2).

^{1}H NMR (400 MHz, $CDCl_3$) δ 7.73 (d, *J* = 8.0 Hz, 2H), 7.31 (d, *J* = 7.9 Hz, 2H), 6.98-6.90 (m, 1H), 6.56 (s, 1H), 6.53 (s, 1H), 5.81 (d, *J* = 15.7 Hz, 1H), 5.17-5.13 (m, 1H), 3.71 (s, 3H), 2.68-2.61 (m, 2H), 2.45 (s, 3H), 2.32-2.26 (m, 2H), 2.12-2.09 (m, 2H), 2.05 (s, 3H), 1.81-1.67 (m, 4H), 1.62-1.49 (m, 2H), 1.58 (s, 3H), 1.25 (s, 3H).

^{13}C NMR (100 MHz, $CDCl_3$) δ 167.4, 150.8, 149.4, 145.2, 141.7, 134.0, 133.1, 129.8 (2C), 128.8 (2C), 127.7, 125.4, 122.1, 121.3, 121.2, 120.4, 76.3, 51.6, 40.0, 38.1, 31.1, 30.9, 24.2, 22.5, 22.3, 21.9, 16.3, 16.0.

IR (neat) *vmax* 2925, 2852, 1722, 1473, 1450, 1371, 1189, 1176, 1093, 984 cm^{-1}.

---

p4

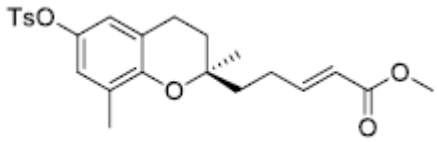

Mw = 444.5405 g/mol

methyl(2*E*)-5-[(2*R*)-2,8-dimethyl-6-[(4-methylbenzenesulfonyl)oxy]-3,4-dihydro-2H-1-benzopyran-2-yl]pent-2-enoate

Yellow oil; 49% yield; Rf = 0.44 (cyclohexane/ethyl acetate 7:2).

^{1}H NMR (400 MHz, $CDCl_3$) δ 7.73 (d, *J* = 8.1 Hz, 2H), 7.31 (d, *J* = 8.0 Hz, 2H), 7.03-6.96 (m, 1H), 6.57 (s, 1H), 6.53 (s, 1H), 5.83 (d, *J* = 15.6 Hz, 1H), 3.72 (s, 3H), 2.73-2.61 (m, 2H), 2.45 (s, 3H), 2.39-2.33 (m, 2H), 2.04 (s, 3H), 1.82-1.68 (m, 4H), 1.25 (s, 3H).

^{13}C NMR (100 MHz, $CDCl_3$) δ 167.2, 150.4, 149.4, 145.1, 141.7, 132.9, 129.7 (2C), 128.7 (2C), 127.6, 122.2, 121.1, 121.0, 120.4, 75.8, 51.6, 38.3, 31.1, 26.6, 23.9, 22.3, 21.9, 16.2.

IR (neat) *vmax* 2926, 2851, 1722, 1473, 1371, 1189, 1177, 1094, 984 cm^{-1}.

General procedure of deprotection of new δT3 derivatives

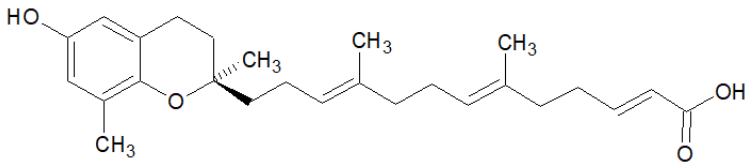

(2*E*,6*E*,10*E*)-13-[(2*R*)-6-hydroxy-2,8-dimehyl-3,4-dihydro-2H-1-benzopyran-2-yl]-6,10-dimethyltrideca-2,6,10-trienoic acid

Mw = 344.4446 g/mol

1st step:

p3 (26.3 mg; 0.0513 mmol; 1 eq.) was dissolved in 4 mL of mixture of THF/MeOH/H_2O (3:1:1) and LiOH (5.38 mg; 0.223 mmol; 4.33 eq.) was added. The reaction was stirred at 40°C for 17 hours. The completion of reaction was checked by TLC (UV light and CAM stain) with PE/Ac/DCM (7:2:1) as a mobile phase. The reaction was quenched with 10% hydrochloric acid, extracted three times with ethyl acetate, then pooled organic layers were washed twice with water and once with brine, dried over anhydrous sodium sulfate and filtered. The solvent was removed under reduced pressure. Yields of desired product was 90 %.

2nd step:

Product from 1st step of deprotection (22.4 mg; 0.0464 mmol; 1 eq.) was dissolved in 5 mL MeOH and KOH (2M aq. sol.) (561.1 mg; 10 mmol) was added. The reaction was stirred 6 hours at 70°C and 12 hours without heating (overnight). The completion of reaction was checked by TLC (UV light and CAM stain) with PE/Ac/DCM (7:2:1) as a mobile phase. The reaction was quenched with 10% hydrochloric acid, extracted three times with diethyl ether, then pooled organic layers were washed twice with water and once with brine, dried over anhydrous sodium sulfate and filtered. The solvent was removed under reduced pressure. The purification by preparative TLC on silica gel was carried out. The product was obtained in 16% yield.

Light yellow oil; 16% total yield; Rf = 0.53 (petroleum ether/acetone/dichloromethane 7:2:1)

^{1}H NMR (400 MHz, $CDCl_3$) δ 7.09 – 7.02 (m, 1H), 6.48 (s, 1H), 6.38 (s, 1H), 5.86 – 5.77 (m, 1H), 5.16 – 5.09 (m, 2H), 2.72 – 2.66 (m, 2H), 2.35 – 2.23 (m, 2H), 2.16 – 2.01 (m, 10H), 1.98 – 1.93 (m, 2H), 1.82 – 1.71 (m, 2H), 1.64 – 1.52 (m, 8H), 1.26 (s, 4H).

^{13}C NMR (100 MHz, $CDCl_3$) δ 171.64, 152.31, 147.84, 146.06, 134.95, 133.42, 127.49, 125.48, 124.64, 121.35, 120.59, 115.77, 112.73, 75.44, 39.60, 39.51, 37.83, 31.48, 31.01, 26.52, 24.28, 22.59, 22.29, 16.23, 16.09, 15.96.

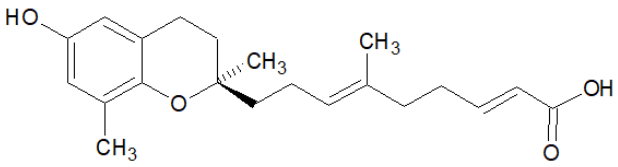

(2*E*,6*E*)-9-[(2*R*)-6-hydroxy-2,8-dimethyl-3,4-dihydro-2H-1-benzopyran-2-yl]-6-methylnona-2,6-dienoic acid

Mw = 414.5616 g/mol

1st step:

p2 (40 mg; 0.0689 mmol; 1 eq.) was dissolved in 5.4 mL of mixture of THF/MeOH/H_2O (3:1:1) and LiOH (7.14 mg; 0.298 mmol; 4.33 eq.) was added. The reaction was stirred at 40°C for 20 hours. The reaction was evaluated by TLC (UV light and CAM stain) with eluents PE/Ac/DCM (7:2:1). The reaction was quenched with 10% HCl, extracted three times with ethyl acetate, then pooled organic layers were washed with water and brine, dried over anhydrous sodium sulfate and filtered. The solvent was removed under reduced pressure. Yields of desired product was 90 %.

2nd step:

Product from 1st step of deprotection (37.1 mg; 0.0674 mmol; 1 eq.) was dissolved in 8 mL MeOH and KOH (2M aq. sol.) (897.76 mg; 16 mmol) was added. The reaction was stirred 6 hours at 70°C. The reaction was evaluated by TLC (UV light and CAM stain) with eluents PE/Ac/DCM (7:2:1). The reaction was quenched with 10% HCl, extracted three times with diethyl ether, then pooled organic layers were washed with water and brine, dried over anhydrous sodium sulfate and filtered. The solvent was removed under reduced pressure. The purification by preparative TLC on silica gel was carried out. The product was obtained in 31% yield.

Light yellow oil; 31% total yield; Rf = 0.47 (petroleum ether/acetone/dichloromethane 7:2:1)

^{1}H NMR (400 MHz, $CDCl_3$) δ 7.12 – 6.96 (m, 1H), 6.48 (s, 1H), 6.38 (s, 1H), 5.84 – 5.78 (m, 1H), 5.19 – 5.13 (m, 1H), 2.71 – 2.65 (m, 2H), 2.35 – 2.29 (m, 2H), 2.17 – 2.07 (m, 7H), 1.79 – 1.72 (m, 2H), 1.69 – 1.47 (m, 6H), 1.26 (s, 4H).

^{13}C NMR (100 MHz, CDCl3) δ 171.38, 152.13, 147.83, 146.06, 133.51, 127.49, 125.74, 121.35, 120.64, 115.76, 112.73, 75.37, 39.57, 37.84, 31.51, 30.91, 24.16, 22.57, 22.25, 16.22, 15.91.

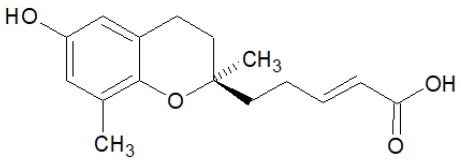

(2*E*)-5-[(2*R*)-6-hydroxy-2,8,-dimethyl-3,4-dihydro-2H-1benzopyran-2-yl]pent-2-enoic acid

Mw = 276.3276 g/mol

1st step:

p2 (80 mg; 0.180 mmol; 1 eq.) was dissolved in 10.6 mL of mixture of THF/MeOH/H_2O (3:1:1) and LiOH (18.66 mg; 0.779 mmol; 4.33 eq.) was added. The reaction was stirred at 40°C for 4 hours. The completion of reaction was checked by TLC (UV light and CAM stain) with PE/Ac/DCM (7:2:1) as a mobile phase. The reaction was quenched with 10% hydrochloric acid, extracted three times with ethyl acetate, then pooled organic layers were washed twice with water and once with brine, dried over anhydrous sodium sulfate and filtered. The solvent was removed under reduced pressure. Yields of desired product was 91 %.

2nd step:

Product from 1st step of deprotection (76.1 mg; 0.183 mmol; 1 eq.) was dissolved in 15 mL MeOH and KOH (2M aq. sol.) (1683.00 mg; 30 mmol) was added. The reaction was stirred 3 hours at 70°C. The completion of reaction was checked by TLC (UV light and CAM stain) with PE/Ac/DCM (7:2:1) as a mobile phase. The reaction was quenched with 10% hydrochloric acid, extracted three times with diethyl ether, then pooled organic layers were washed twice with water and once with brine, dried over anhydrous sodium sulfate and filtered. The solvent was removed under reduced pressure. The purification by column chromatography was carried out. The product was obtained in 17% yield.

Light yellow oil; 17% total yield; Rf = 0.36 (petroleum ether/acetone/dichloromethane 7:2:1)

^{1}H NMR (400 MHz, $CDCl_3$) δ 7.17 – 7.08 (m, 1H), 6.48 (s, 1H), 6.39 (s, 1H), 5.84 (d, J = 15.6 Hz, 1H), 2.77 – 2.64 (m, 2H), 2.44 – 2.38 (m, 2H), 2.11 (s, 3H), 1.87 – 1.60 (m, 5H), 1.26 (s, 4H)**.**

^{13}C NMR (100 MHz, CDCl3) δ 171.54, 152.51, 148.03, 145.72, 127.56, 121.11, 120.51, 115.90, 112.72, 74.87, 37.95, 31.61, 26.78, 23.90, 22.46, 16.11.

The IR spectra of the final deprotected compounds could not be added because of fault of the IR spectrometer.

Appendix

1 Chromatograms of standards

Table 10 and chromatogram 1: Starting compound – TsOδT3.

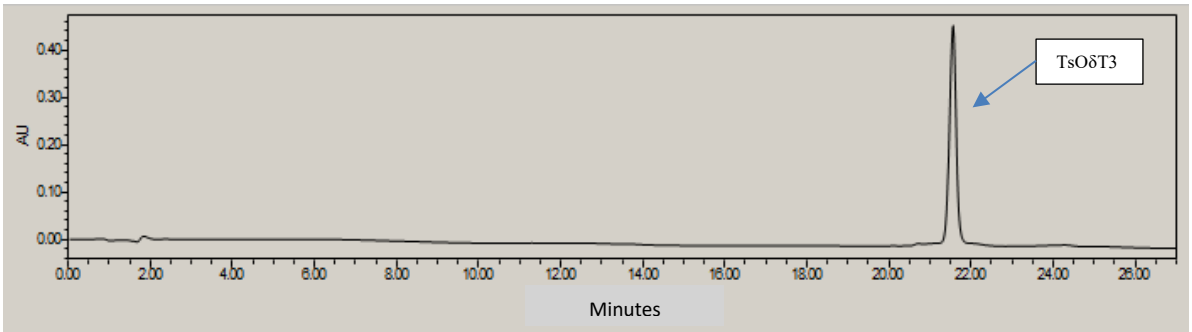

Name	Area (in millions)	Retention time (min)	Purity
TsOδT3	4.28	21.56	99.00 %

Table 11 and chromatogram 2: Product p2.

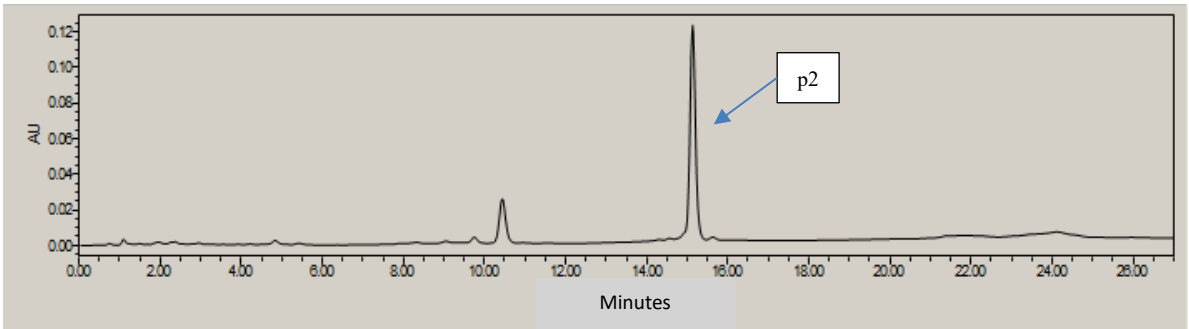

Name	Area (in millions)	Retention time (min)	Purity
p2	1.156	15.23	79.00 %

Table 12 and chromatogram 3: Product p3.

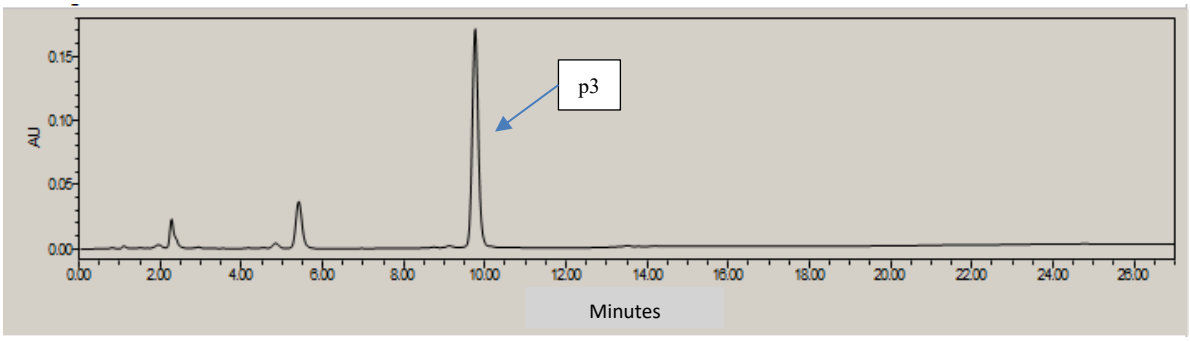

Name	Area (in millions)	Retention time (min)	Purity
p3	1.74	9.81	81.69 %

Table 13 and chromatogram 4: Product p4.

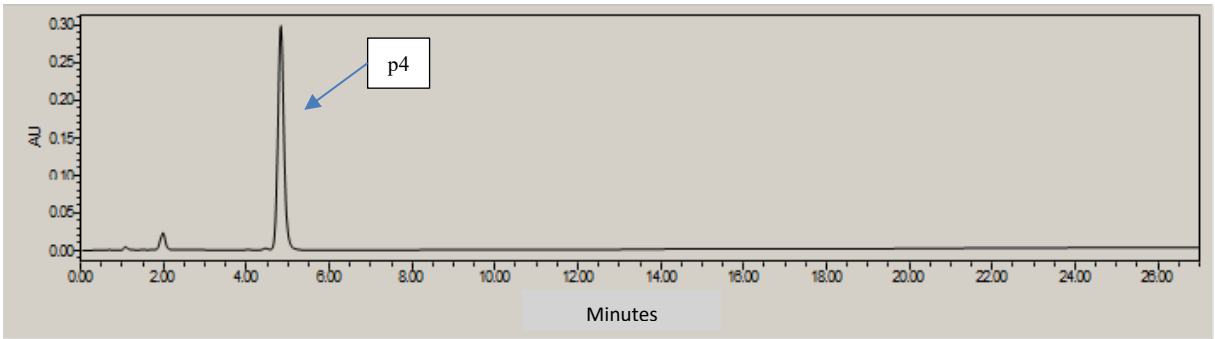

Name	Area (in millions)	Retention time (min)	Purity
p4	2.92	4.90	94.67 %

2 Chromatogram of the highest yield of all products

Table 14 and chromatogram 5: 3-days reaction MS14.

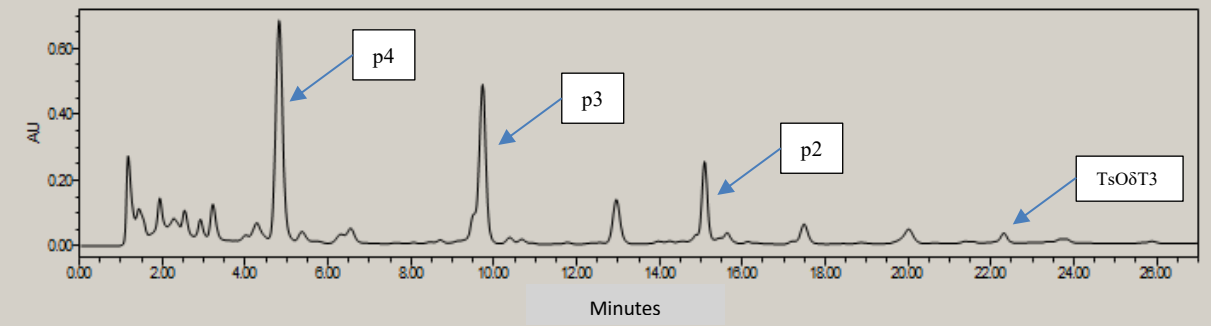

Name	Area (in millions)	Retention time (min)	Estimated yield (%)
TsOδT3	0.09	21.40	nd
p2	2.23	15.09	18
p3	5.55	9.71	31
p4	7.72	4.80	43

3 Chromatograms of balanced ratio of products

Table 15 and chromatogram 6: 1-hour reaction MS45.

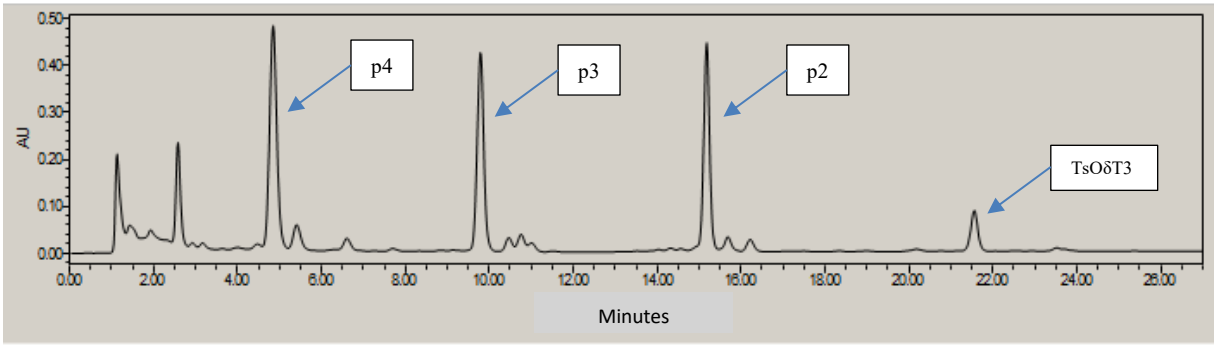

Name	Area (in millions)	Retention time (min)	Estimated yield (%)
TsOδT3	1.00	21.56	nd
p2	4.36	15.18	19
p3	4.65	9.79	22
p4	5.51	4.85	24

Table 16 and chromatogram 7: 3-days reaction MS19.

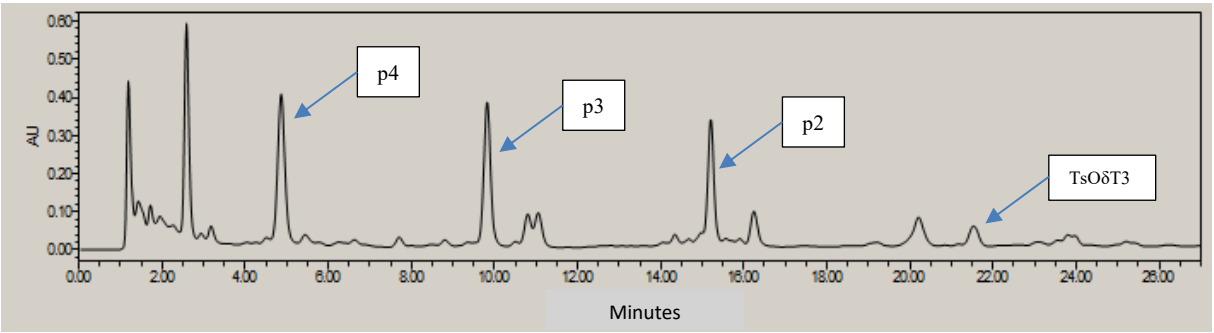

Name	Area (in millions)	Retention time (min)	Estimated yield (%)
TsOδT3	0.70	21.54	nd
p2	2.86	15.20	20
p3	4.05	9.82	22
p4	4.55	4.87	19

4 Table of all performed metathesis reactions during optimization.

Table 17: A summary of all metathesis reactions performed during optimization.

					P2 (%)		P3 (%)		P4 (%)	
SAMPLE	Cat.	T (°C)	Eq. MA	time	Est.	Pur.	Est.	Pur.	Est.	Pur.
MS07	Hg-2	70	1.2	3days	10	N/A	24	N/A	24	N/A
MS07	Hg-2	70	1.2	5days	3	N/A	5	N/A	5	N/A
MS07	Hg-2	70	1.2	7days	3	N/A	6	N/A	6	N/A
MS08	Hg-2	70	0.6	3days	11	N/A	14	N/A	12	N/A
MS08	Hg-2	70	0.6	5days	7	N/A	7	N/A	6	N/A
MS08	Hg-2	70	0.6	7days	5	6	6	7	5	7
MS09	Hg-2	70	0.8	3days	15	N/A	20	N/A	17	N/A
MS09	Hg-2	70	0.8	5days	7	N/A	6	N/A	5	N/A
MS09	Hg-2	70	0.8	7days	8	9	9	8	7	6
MS13	Hg-1	70	1.2	3days	6	N/A	11	N/A	12	N/A
MS13	Hg-1	70	1.2	5days	5	N/A	10	N/A	11	N/A
MS13	Hg-1	70	1.2	7days	4	N/A	8	N/A	9	N/A
MS14	Hg-1	70	2.4	3days	15	15	30	28	33	32
MS15	Hg-1	70	0.6	3days	2	N/A	5	N/A	6	N/A
MS15	Hg-1	70	0.6	5days	2	N/A	4	N/A	5	N/A
MS15	Hg-1	70	0.6	7days	2	4	3	5	4	5
MS16	Hg-1	70	0.8	3days	9	N/A	10	N/A	8	N/A
MS16	Hg-1	70	0.8	5days	8	N/A	10	N/A	8	N/A
MS16	Hg-1	70	0.8	7days	10	10	13	11	10	10
MS17	Hg-2	70	2,4	3days	18	17	31	31	43	40
MS19	Ru-2	70	1.2	3days	20	N/A	22	N/A	19	N/A
MS19	Ru-2	70	1.2	5days	17	N/A	19	N/A	16	N/A
MS19	Ru-2	70	1.2	7days	14	N/A	15	N/A	13	N/A
MS20	Ru-2	70	2.4	3days	10	10	26	27	39	40
MS21	Ru-2	70	0.6	3days	6	N/A	10	N/A	12	N/A
MS21	Ru-2	70	0.6	5days	5	N/A	10	N/A	11	N/A
MS21	Ru-2	70	0.6	7days	4	5	8	7	9	7
MS22	Ru-2	70	0.8	3days	14	N/A	12	N/A	10	N/A
MS22	Ru-2	70	0.8	5days	14	N/A	11	N/A	9	N/A
MS22	Ru-2	70	0.8	7days	12	11	10	9	8	9
MS25	Ru-2	70	2.4	1day	11	12	23	25	39	51
MS26	Hg-2	70	2.4	1day	6	9	18	24	38	45
MS27	Hg-1	70	2.4	1day	26	16	29	27	39	39
MS45	Ru-2	100mw	2.4	1hour	19	N/A	22	N/A	24	N/A
MS45	Ru-2	100mw	2.4	2hour	17	16	18	16	21	20
MS46	Ru-2	120mw	2.4	1hour	12	N/A	15	N/A	13	N/A
MS47	Ru-2	140mw	2.4	1hour	9	N/A	10	N/A	7	N/A
MS51	Hg-1	100mw	2.4	1hour	8	N/A	3	N/A	11	N/A
MS52	Hg-2	100mw	2.4	1hour	nd	N/A	nd	N/A	nd	N/A

References

[1] Watson R. R. and Preedy V. R.: *Tocotrienols: vitamin E beyond tocopherols*. Urbana, IL: AOCS Press, c2009, 3-285. ISBN 978-1-4200-8037-7.

[2] Patel V., Rink C., Khanna S. et al: Tocotrienols: The lesser known form of natural vitamin E. *Indian J. Exp. Biol*. 2011, 49(10), 732–738.

[3] Galli F., Azzi A., Birringer M. et al: Vitamin E: Emerging aspects and new directions. *Free Radical Biol. Med.* 2017, **102**, 16-36.

[4] Ahsan H., Ahad A., Iqbal J. et al: Pharmacological potential of tocotrienols: a review. *Nutr. Metab.* 2014, **11**(1), 52.

[5] Jiang Q.: Natural forms of vitamin E: metabolism, antioxidant, and anti-inflammatory activities and their role in disease prevention and therapy. *Free Radical Biol. Med.* 2014, **72**, 76-90.

[6] Mene-Saffrané L.: Vitamin E Biosynthesis and Its Regulation in Plants. *Antioxidants*. 2018, **7**(1), 2.

[7] Hofius D., Sonnewald U., Hunter S. C. et al: Vitamin E biosynthesis: biochemistry meets cell biology. *Trends Plant Sci.* 2003, **8**(1), 6-8.

[8] Yang W., Cahoon R. E., Hunter S. C. et al: Vitamin E biosynthesis: functional characterization of the monocot homogentisate geranylgeranyl transferase. *Plant J.* 2011, **65**(2), 206-217.

[9] Fritsche S., Wang X. and Jung C.: Recent Advances in our Understanding of Tocopherol Biosynthesis in Plants: An Overview of Key Genes, Functions, and Breeding of Vitamin E Improved Crops. *Antioxidants*. 2017, **6**(4), 99.

[10] Falk J. and Munné-Bosch S.: Tocochromanol functions in plants: antioxidation and beyond. *J. Exp. Bot.* 2010, **61**(6), 1549-1566.

[11] Ajjawi I. and Shintani D.: Engineered plants with elevated vitamin E: a nutraceutical success story. Trends Biotechnol. 2004, **22**(3), 104-107.

[12] Cardenas E. and Ghosh R.: Vitamin E: A dark horse at the crossroad of cancer management. *Biochem. Pharmacol*. 2013, **86**(7), 845-852.

[13] Schmolz L., Lorkowski S., Birringer M. et al: Complexity of vitamin E metabolism. *World J. Biol. Chem.* 2016, **7**(1), 14-43.

[14] Institute of Medicine. *Dietary reference intakes for vitamin C, vitamin E, selenium, and carotenoids*. Washington, D.C.: National Academy Press, c2000, 186-281. ISBN 03-090-6949-1.

[15] Manolescu B., Atanasiu V., Cercasov C. et al: So many options but one choice: the human body prefers α-tocopherol. A matter of stereochemistry. *J. Med. Life.* 2008, **1**(4), 376-382.

[16] Shahidi F., De Camargo A.: Tocopherols and Tocotrienols in Common and Emerging Dietary Sources: Occurrence, Applications, and Health Benefits. *Int. J. Mol. Sci.* 2016, **17**(10), 17-45.

[17] Sen C. K., Khanna S., Rink C. et al: Tocotrienols: The Emerging Face of Natural Vitamin E. *Vitam. Horm*. 2007, **17**(10), 203-261.

[18] United States Department of Agriculture, Agricultural Research Service. USDA Food Composition Databases [online database], [retrieved 8. 12. 2018]. Available at: https://ndb.nal.usda.gov/ndb/nutrients/report/nutrientsfrm?max=25&offset=0&totCount=0&nutrient1=323&nutrient2=&nutrient3=&subset=0&sort=c&measureby=g.

[19] Theriault A., Chao J.T., Wang Q. et al: Tocotrienol: A Review of Its Therapeutic Potential. *Clin. Biochem*. 1999, **32**(5), 309-319.

[20] Vilar D. A. and Vilar M. S. A. et al: Traditional Uses, Chemical Constituents, and Biological Activities of Bixa orellana L.: A Review. *Sci. World J.* 2014, **2014**, 11.

[21] Bruneton J.: *Pharmacognosie: Phytochimie, Plantes Médicinales*. 5. Paris: Tec & Doc Lavoisier, 2016, 141-145, 777. ISBN 978-2-7430-2165-8.

[22] Stohs S. J.: Safety and Efficacy of *Bixa orellana* (Achiote, Annatto) Leaf Extracts. *Phytother. Res.* 2014, **28**(7), 956-960.

[23] Moraes M. N., Zabot G. L. and. Meireles M. A. A.: Extraction of tocotrienols from annatto seeds by a pseudo continuously operated SFE process integrated with low-pressure solvent extraction for bixin production. *J. Supercrit. Fluid.* 2015, **96**(7), 262-271.

[24] Maki K.C., Geohas J. G., Dicklin M. R. et al: Safety and lipid-altering efficacy of a new omega-3 fatty acid and antioxidant-containing medical food in men and women with elevated triacylglycerols. *Prostaglandins Leukot. Essent. Fatty Acids*. 2015, **99**, 41–46.

[25] Vik A., James A. and Gundersen L. L.: Screening of terpenes and derivatives for antimycobacterial activity; identification of geranylgeraniol and geranylgeranyl acetate as potent inhibitors of Mycobacterium tuberculosis in vitro. *Planta Med*. 2007, **73**(13), 1410–1412.

[26] Picture taken from: Bixa orellana. In: *Horticultural Impex* [online]. Uttarakhand, India, 2012 [retrieved 22. 6. 2019]. Available at: http://www.ehorticulture.com/tree-plants-seeds/medicinal-plants/bixa-orellana-detail.html.

[27] Nagendran B., Unnithan U. R., Choo Y. M. et al: Characteristics of Red Palm Oil, a Carotene- and Vitamin E-rich Refined Oil for Food Uses. *Food Nutr. Bull.* 2000, *21*(2), 189–194.

[28] Mancini A., Imperlini E., Nigro E. et al: Biological and Nutritional Properties of Palm Oil and Palmitic Acid: Effects on Health. *Molecules*. 2015, **20**(9), 17339-17361.

[29] Netscher, T., F. Mazzini and R. Jestin: Tocopherols by Hydride Reduction of Dialkylamino Derivatives. *Eur. J. Org. Chem.*, 2007, **2007**, 1176–1183.

[30] Fitzherbert E., Struebig M., Morel A. et al: How will oil palm expansion affect biodiversity? *Trends Ecol. Evol*. 2008, **23**(10), 538-545.

[31] Butler R. A., Koh L. P. and Ghazoul J.: REDD in the red: palm oil could undermine carbon payment schemes. *Conserv. Lett.* 2009, **2**(2), 67-73.

[32] Corley R. H. V.: How much palm oil do we need? *Environ. Sci. Policy.* 2009, **12**(2), 134-139.

[33] Wu Y., Xiao N., Yu L. et al: Combination Patterns of Major R Genes Determine the Level of Resistance to the M. oryzae in Rice (*Oryza sativa L.*): A Versatile Source for Edible and Industrial Applications. *PLoS one*. 2015, **10**(6), 2606-2618.

[34] Pal Y. P. and Pratap A. P.: Rice Bran Oil: A Versatile Source for Edible and Industrial Applications. *J. Oleo Sci.* 2017, **66**(6), 551-556.

[35] Qureshi A. A., Salser W. A., Parmar R. et al: Novel Tocotrienols of Rice Bran Inhibit Atherosclerotic Lesions in C57BL/6 ApoE-Deficient Mice: A Versatile Source for Edible and Industrial Applications. *J. Nutr.* 2001, **131**(10), 2606-2618.

[36] Picture taken from: Effect of rice bran application for eco- friendly weed control in Bangladesh. In: *INTERNATIONAL NETWORK FOR NATURAL SCIENCES* [online]. 2014 [retrieved 22. 6. 2019]. Available at: https://innspubnet.wordpress.com/2015/06/23/effect-of-rice-bran-application-for-eco-friendly-weed-control-growth-and-yield-of-lowland-rice-in-bangladesh/.

[37] Hemshekhar M., Sunitha K., Santhosh M. S. et al: An overview on genus garcinia: phytochemical and therapeutical aspects. *Phytochem. Rev*. 2011, **10**(3), 325-351.

[38] Nimanthika W. J. and Kaththriarachchi H. S.: Systematics of genus *Garcinia L*. (*Clusiaceae*) in Sri Lanka: new insights from vegetative morphology. *J. Natl. Sci. Found. Sri.* 2010, **38**(1), 29-44.

[39] Farombi E. O. and Owoeye O.: Antioxidative and Chemopreventive Properties of Vernonia amygdalina and Garcinia biflavonoid: new insights from vegetative morphology. *Int. J. Environ. Res. Public Health.* 2011, **8**(6), 2533-2555.

[40] Adegboye M. F., Akinpelu D. A. and Okoh A. I.: The bioactive and phytochemical properties of *Garcinia kola (Heckel)* seed extract on some pathogens. *Afr. J. Biotechnol.* 2008, **7**(21), 3934-3938.

[41] Picture taken from: Kola Nut Powder. In: *Zion Herbals: Premium Botanicals* [online]. [retrieved 23. 6. 2019]. Available at : https://zionherbals.com/product/kola-nut-powder/#prettyphoto[gallery]/0/

[42] Kenne Michel T., Arua Ottoh A., Christopher Emeka Chukwunonye U. et al: Bio-flavonoids and Garcinoic Acid from *Garcinia kola* seeds with Promising Anti-Inflammatory Potentials. *Pharmacognosy Journal*. 2015, **8**(1), 56-58.

[43] K. Terashima, T. Shimamamura, M. Tanabayashi et al: Constituents of the Seeds of *Garcinia kola*: Two New Antioxidants, Garcinoic Acid and Garcinal. *Heterocycles*, 1997, **45**, 1560–1566.

[44] Lavaud A., Richomme P., Gatto J. et al: A tocotrienol series with an oxidative terminal prenyl unit from *Garcinia amplexicaulis*. *Phytochemistry*. 2015, **109**(21), 103-110.

[45] Grison C., Escande V. and Biton J.: *Ecocatalysis: A New Integrated Approach to Scientific Ecology*. 1. ISTE Press - Elsevier, 2015, 35. ISBN 978-1785480300.

[46] Picture taken from: *Garcinia amplexicaulis*. In: *Les galeries photos des plantes et de jardins* [online]. 2015 [retrieved 23. 6. 2019]. Available at: http://gardenbreizh.org/photos/Ben152/photo-691434.html.

[47] Niki E.: Evidence for beneficial effects of vitamin E. *Korean J. Intern. Med*. 2015, **30**(5), 571-579.

[48] Traber M. G. and Stevens J. F.: Vitamin C and E: Beneficial effect from a mechanistic perspective. *Free Radic. Biol. Med.*, 2011, 51, 1000-1013.

[49] Qureshi A. A., Burger W. C., Peterson D. M. et al: The Structure of an Inhibitor of Cholesterol Biosynthesis Isolated from Barley. *J. Biol. Chem.* 1986, **261**(23), 10544-10550.

[50] Sen C. K., Khana S. and Roy S.: Tocotrienols in health and disease: the other half of the natural vitamin E family. *Mol Aspects Med*. 2007, **28**(5-6), 692–728.

[51] Meganathan P., Fu J. Y., Sak K. et al: Biological Properties of Tocotrienols: Evidence in Human Studies. *Int. J. Mol. Sci.* 2016, **17**(11), 259-272.

[52] Stephens N., Parsons A., Schofield P. et al: Randomised controlled trial of vitamin E in patients with coronary disease. *Clin. Sci.* 1996, **91**, 16-17.

[53] Esterbauer H., Dieber-Rotheneder M., Striegl G. et al: Role of vitamin E in preventing the oxidation of low-density lipoproteins. *Am. J. Clin. Nutr.* 1991, **53**, 314–321.

[54] Salonen J. T, Ylä-Herttuala S., Yamamoto R. et al: Autoantibody against oxidized LDL and progression of carotid atherosclerosis. *Lancet Lond. Engl.* 1992, **339**, 883–887.

[55] Salonen J. T., Salonen R., Penttilä I. et al: Serum fatty acids, apolipoproteins, selenium and vitamins antoxidants and the risk of death from coronary artery diasease *Am. J. Cardiol.* 1985, **56**, 226–231.

[56] Kok F. J., de Bruijn A. M, Vermeeren R.et al: Serum selenium, vitamin antioxidants, and cardiovascular mortality. *Am. J. Clin. Nutr.* 1987, **45**, 462–468.

[57] Wong W. Y., Ward L. C., Fong C. W. et al: Anti-inflammatory γ- and δ-tocotrienols improve cardiovascular, liver and metabolic function in diet-induced obese rats: Evidence in Human Studies. *Eur. J. Nutr*. 2017, **56**(1), 133-150.

[58] Tomeo A. C., Geller M., Watkins T. R. et al: Antioxidant effect of tocotrienols in patients with hyperlipidemia and carotic stenosis. *Lipids*, 1995, **30**, 1179–1183.

[59] Sailo B. L., Banik K., Padmavathi G. et al: Tocotrienols: The promising analogues of vitamin E for cancer therapeutics. *Pharmacol. Res*. 2018, **130**(6), 259-272.

[60] Aggarwal V., Kashyap D., Sak K. et al: Molecular Mechanisms of Action of Tocotrienols in Cancer: Recent Trends and Advancements*. Int. J. Mol. Sci.* 2019, **20**(3), 259-272.

[61] Comitato R., Ambra R. and Virgili F.: Tocotrienols: A Family of Molecules with Specific Biological Activities. *Antioxidants*. 2017, **6**(4), 93.

[62] Osakada F., Hashino A., Kume T. et al: A-Tocotrienol provides the most potent neuroprotection among vitamin E analogs on cultured striatal neurons. *Neuropharmacology*. 2004, **47**(6), 904-915.

[63] Nesaretnam K., Meganathan P. Fong C. W. et al: Tocotrienols: inflammation and cancer. *Ann. N. Y. Acad. Sci.* 2011, **1229**(1), 18-22.

[64] Reddanna P., Whelan J., Maddipati K. R. et al: Purification of arachidonate 5-Lipoxygenase from potato tubers. *Methods Enzymol*. 1990, 187, 268-77.

[65] Jiang Q., Yin X., Lill M. A. et al: Long-chain carboxychromanols, metabolites of vitamin E, are potent inhibitors of cyclooxygenases. *Proc. Natl. Acad. Sci.* 2008, 105, 20464–20469.

[66] Charlier C. and Michaux C.: Dual inhibition of cyclooxygenase-2 (COX-2) and 5-lipoxygenase (5-LOX) as a new strategy to provide safer non-steroidal anti-inflammatory drugs. *Eur. J. Med. Chem.* 2003, **38**, 645–659.

[67] Pein H., Ville A., Pace S. et al: Endogenous metabolites of vitamin E limit inflammation by targeting 5-lipoxygenase: inflammation and cancer. *Nat. Commun*. 2018, **9**(1), 18-22.

[68] Chen L., Deng H., Cui H. et al: Inflammatory responses and inflammation-associated diseases in organs. *Oncotarget*. 2018, **9**(6), 7204-7218.

[69] Muid S., Froemming G. R. A., Rahman T. et al: Delta- and gamma-tocotrienol isomers are potent in inhibiting inflammation and endothelial activation in stimulated human endothelial cells: inflammation and cancer. *Ann. N. Y. Acad. Sci.* 2016, **60**(1), 18-22.

[70] Chen S.: Natural Products Triggering Biological Targets - A Review of the Anti-Inflammatory Phytochemicals Targeting the Arachidonic Acid Pathway in Allergy Asthma and Rheumatoid Arthritis. *Curr. Drug Targets*. 2011, **12**(3), 288-301.

[71] Zeldin D. C.: Epoxygenase Pathways of Arachidonic Acid Metabolism. *J. Biol. Chem*. 2001, **276**(39), 36059-36062.

[72] Ricciotti E. and Fitzgerald G. A.: Prostaglandins and Inflammation. *Arterioscler. Thromb. Vasc. Biol.* 2011, **31**(5), 986-1000.

[73] Abdulkhaleq L. A.,Assi M. A., Abdullah R. et al: The crucial roles of inflammatory mediators in inflammation: A review. *Vet. World*. 2018, **11**(5), 627-635.

[74] Samuelsson, B.: Arachidonic acid metabolism: Role in inflammation. Z. Rheumatol. 1991, 50, Suppl 1, 3-6.

[75] Xie W. L., Chipman J. G., Robertson D. L. et al: Expression of mitogen-resposive gene encoding prostaglandin synthase is regulated by mRNA splicing. *Proc. Natl. Acad. Sci. U. S. A.* 1991, **88**, 2692–2696.

[76] Meirer K., Steinhilber D. and Proschak E.: Inhibitors of the Arachidonic Acid Cascade: Interfering with Multiple Pathways. *Basic Clin. Pharmacol. Toxicol.* 2014, **114**(1), 83-91.

[77] Kurumbail R. G., Kiefer J. R. and Marnett L. J.: Cyclooxygenase enzymes: catalysis and inhibition. *Curr. Opin. Struct. Biol*. 2001, **11**(6), 752-760.

[78] Smith W. L., DeWitt D. L. and Garavino R. M.: Cyclooxygenases: structural, cellular, and molecular biology. *Annu. Rev. Biochem.* 2000, 69, 145-182.

[79] Mowry J. B., Spyker D. A., Brooks D. E.et al: 2015 Annual Report of the American Association of Poison Control Centers' National Poison Data System (NPDS): 33rd Annual Report. *Clin. Toxicol. Phila. Pa.* 2016, **54**(10), 924–1109.

[80] Pilotto A., Franceschi M., Leandro G.et al: The effect of Helicobacter pylori infection on NSAID-related gastrointestinal damage in the elderly. *Eur. J. Gastroenterol. Hepatol.* 1997, **9**, 951–956.

[81] Clive D. M. and Stoff J. S.: Renal syndromes associated with nonsteroidal antiinflammatory drugs. *N. Engl. J. Med.*, 1984, **310**(9), 563–572.

[82] Day R. O. and Graham G. G.: The vascular effects of COX-2 selective inhibitors. *Aust. Prescr.* 2004, **27**(6), 142-145.

[83] Masferrer J. L., Zweifel B. S., Manning P. T et al: Selective inhibition of inducible cyclooxygenase 2 in vivo is inflammatory and nonulcerogenic. *Proc. Natl. Acad. Sci. U. S. A.*, 1994, **91**(8), 3228–3232.

[84] Shi S. and Klotz U.: Clinical use and pharmacological properties of selective COX-2 inhibitors. *Eur. J. Clin. Pharmacol.* 2008, **64**, 233–252.

[85] *Lipoxygenases in inflammation*. 1. New York, NY: Springer Berlin Heidelberg, 2016, 7-101. ISBN 978-3-319-27764-6.

[86] Werz O.: Inhibition of 5-Lipoxygenase Product Synthesis by Natural Compounds of Plant Origin. *Planta Med*. 2007, **73**(13), 1331-1357.

[87] Gilbert N. C., Bartlett S. G., Waight M. T. et al: The Structure of Human 5-Lipoxygenase, *Science*, 2011, **331**(6014), 217–219.

[88] Still W. C., Kahn M. and Mitra A.: Rapid chromatographic technique for preparative separations with moderate resolution. *J. Org. Chem.* 1978, **43**(14), 2923-2925.

[89] Personal interview with Helesbeux J. J., SONAS, Angers, September – December 2018.

[90] Singh O. M.: Metathesis Catalysts: Historical Perspective, Recent developments and Practical applications. *J. Sci. Ind. Res*. 2006, **65**, 957-965.

[91] Montgomery T. P., Ahmed T. S. and Grubbs R. H.: Stereoretentive Olefin Metathesis: An Avenue to Kinetic Selectivity. *Angew. Chem. Int. Ed. Engl*. 2017, **56**(37), 11024-11036.

[92] Mukherjee N., Planer S. and Grela K.: Formation of tetrasubstituted C–C double bonds via olefin metathesis: challenges, catalysts, and applications in natural product synthesis. *Org. Chem. Front*. 2018, **5**(3), 494-516.

[93] Grubbs R. H., Wenzel A. G. and Chatterjee A. K.: Olefin Metathesis. *Comprehensive Organometallic Chemistry III* [online]. Elsevier, 2007, 11, 179-205 [retrieved 27. 6. 2019].

[94] Ogba O. M., Warner N. C., O'Leary D. J. et al: Recent advances in ruthenium-based olefin metathesis. *Chem. Soc. Rev*. 2018, **47**(12), 4510-4544.

[95] Murdzek J. S. and Schrock R. R.: Well-characterized olefin metathesis catalysts that contain molybdenum. *Organometallics*, 1987, 6, 1373-1374.

[96] Schrock R. R., Murdzek J. S., Barzan G. C. et al: Synthesis of molybdenum imido alkylidene complexes and some reactions involving acyclic olefins. *J. Am. Chem. Soc.* 1990, 112, 3875-3886.

[97] Nguyen S. T., Johson L. K., Grubbs R. H. et al: Ringopening metathesis polymerization (ROMP) of norbornene by a Group VIII carbene complex in protic media. *J. Am. Chem. Soc.*1992, 114, 3974-3975.

[98] Sanford M. S., Ulman M. and Grubbs R. H.: New insights into the mechanism of Ruthenium catalyzed olefin metathesis reactions, *J. Am. Chem. Soc.* 2001, 123, 749-750.

[99] Garber S. B., Kingsbury J. S., Gray B. L. et al: Efficient and Recyclable Monomeric and Dendritic Ru-Based Metathesis Catalysts. *J. Am. Chem. Soc.* 2000, **122**(34), 8168–8179.

[100] Structure of Ru-2 catalyst taken from: Grubbs Catalyst® 2nd Generation. In: *Merck KGaA: Sigma-Aldrich* [online]. 2019 [retrieved 8. 8. 2019]. Available at: https://www.sigmaaldrich.com/catalog/product/aldrich/569747?lang=en®ion=CZ.

[101] Structure of Hg-1 catalyst taken from: Hoveyda-Grubbs Catalyst® 2nd Generation. In: *Merck KGaA: Sigma-Aldrich* [online]. 2019 [retrieved 8. 8. 2019]. Available at: https://www.sigmaaldrich.com/catalog/product/aldrich/569755?lang=en®ion=CZ.

[102] Structure of Hg-2 catalyst taken from: Grubbs Catalyst® C711. In: *Merck KGaA: Sigma-Aldrich* [online]. 2019 [retrieved 8. 8. 2019]. Available at: https://www.sigmaaldrich.com/catalog/product/aldrich/729345?lang=en®ion=CZ.

[103] Kappe C.O. and Stadler A.: *Microwaves in organic and medicinal chemistry*. Weinheim: Wiley-VCH, c2005, 1-24. ISBN 978-3-527-31210-8.

[104] *Microwave-assisted synthesis* [online]. Anton Paar, 2019 [retrieved 28. 6. 2019]. Available at: https://wiki.anton-paar.com/en/microwave-assisted-synthesis/.

[105] Lindström P., Tierney J., Wathey B. et al: Microwave assisted organic synthesis – a review. *Tetrahydron*. 2001, 57, 9225-9283.

[106] Kappe C. O.: Controlled Microwave Heating in Modern Organic Synthesis. *Angew. Chem. Int. Ed. Engl.* 2004, 43(46), 6250-6284.

Abstract

Many studies highlighted the biological potential of vitamin E, especially tocotrienols (T3), a vitamin E subfamily, particularly in the field of cardiovascular diseases and chronic inflammation. A pharmacophore based virtual screening of these substances against various antiinflammatory targets showed that this class could be considered as potential inhibitors of 5-lipoxygenase, a key enzyme in the biosynthesis of chemoattractant and vasoactive leukotrienes. Consequently, this screening was confirmed by *in vitro* assays.

However, usual natural sources of T3 provide complex mixtures involving particularly challenging purification processes. Thus, this work aims at designing and optimizing efficient semisynthesis towards pharmacologically relevant T3 derivatives were developed from δ-tocotrienol, the main T3 isolated from *Bixa orellana* seeds, a renewable and easily available vegetal source from tropical regions, analyzed mainly by HPLC chromatography. Verification of the most effective reaction conditions of semisynthesis and synthesis another potential inhibitors of 5-LOX based on tocotrienols' structure are the following aims of the work.

During this study, the semisynthesis based on δ-tocotrienol was completely optimized and 3 new T3 derivatives were synthesized and fully characterized. Unfortunately, after several attempts, these most efficient metathesis reaction conditions were not applicable to semisynthesis based on different analogues of T3 and δ-garcinoic acid.

Key words: tocotrienols; 5-LOX inhibition; semisynthesis; optimization

The study was supported by Erasmus+ programme and SVV 260 416.

Abstrakt

Biologický potenciál vitamínu E, hlavně podskupiny tokotrienolů (T3), byl podložen mnoha studiemi již dříve, jedná se zejména o jeho aktivní působení v oblasti kardiovaskulárních onemocnění a chronického zánětu. *In silico* screening prokázal, že tato skupina může být považována za potenciální inhibitory 5-lipoxygenázy - klíčového enzymu v biosyntéze vazoaktivních leukotrienů. Tento screening byl následně potvrzen i *in vitro* testy.

Obvyklé přírodní zdroje T3 však poskytují složité směsi sloučenin, které vyžadují poměrně náročné způsoby purifikace. Proto cílem této práce je navrhnout a optimalizovat účinnou semisyntézu vedoucí k farmakologicky relevantním derivátům T3 založenou na výchozí sloučenině δ-tokotrienolu. Tento izomer je majoritním T3 izolovaným ze semen *Bixa orellana* - obnovitelného a snadno dostupného rostlinného zdroje. Při této optimalizaci byla využita primárně HPLC analýza. Dalším cílem práce je ověření a vyzkoušení nejúčinnějších reakčních podmínek pro reakce dalších T3 analogů a semisyntéza dalších potenciálních inhibitorů 5-LOX založených na strukturní podobnosti s T3.

Během této práce byla zcela optimalizována semisyntéza s využitím δ-tokotrienolu jako výchozí sloučeniny, a zároveň byly syntetizovány 3 nové deriváty T3, které byly zcela charakterizovány. Po několika pokusech s dalšími reaktanty bylo zjištěno, že tyto nejúčinnější reakční podmínky nejsou využitelné pro semisyntézu dalších derivátů T3 a kyseliny δ-garciniové.

Klíčová slova: tokotrienoly; inhibice 5-LOX; semisyntéza; optimalizace

Práce byla umožněna díky programu Erasmus+ a SVV 260 416.